



Heavy Tails in SGD and Compressibility of Overparametrized Neural Networks

Melih Barsbey, Milad Sefidgaran, Murat A Erdogdu, Gael Richard, Umut Şimşekli

► To cite this version:

Melih Barsbey, Milad Sefidgaran, Murat A Erdogdu, Gael Richard, Umut Şimşekli. Heavy Tails in SGD and Compressibility of Overparametrized Neural Networks. 35th Conference on Neural Information Processing Systems (NeurIPS), Dec 2021, Online, United States. hal-03413484

HAL Id: hal-03413484

<https://telecom-paris.hal.science/hal-03413484>

Submitted on 3 Nov 2021

HAL is a multi-disciplinary open access archive for the deposit and dissemination of scientific research documents, whether they are published or not. The documents may come from teaching and research institutions in France or abroad, or from public or private research centers.

L'archive ouverte pluridisciplinaire **HAL**, est destinée au dépôt et à la diffusion de documents scientifiques de niveau recherche, publiés ou non, émanant des établissements d'enseignement et de recherche français ou étrangers, des laboratoires publics ou privés.

Heavy Tails in SGD and Compressibility of Overparametrized Neural Networks

Melih Barsbey*

Boğaziçi University
melih.barsbey@boun.edu.tr

Milad Sefidgaran*

LTCI, Télécom Paris, Institut Polytechnique de Paris
milad.sefidgaran@telecom-paris.fr

Murat A. Erdogdu

University of Toronto & Vector Institute
erdogdu@cs.toronto.edu

Gaël Richard

LTCI, Télécom Paris, Institut Polytechnique de Paris
gael.richard@telecom-paris.fr

Umut Şimşekli

INRIA & ENS – PSL Research University
umut.simsekli@inria.fr

Abstract

Neural network compression techniques have become increasingly popular as they can drastically reduce the storage and computation requirements for very large networks. Recent empirical studies have illustrated that even simple pruning strategies can be surprisingly effective, and several theoretical studies have shown that compressible networks (in specific senses) should achieve a low generalization error. Yet, a theoretical characterization of the underlying causes that make the networks amenable to such simple compression schemes is still missing. In this study, focusing our attention on stochastic gradient descent (SGD), our main contribution is to link compressibility to two recently established properties of SGD: (i) as the network size goes to infinity, the system can converge to a *mean-field* limit, where the network weights behave independently [DBDF20], (ii) for a large step-size/batch-size ratio, the SGD iterates can converge to a *heavy-tailed* stationary distribution [HM20, GŞZ21]. Assuming that both of these phenomena occur *simultaneously*, we prove that the networks are guaranteed to be ' ℓ_p -compressible', and the compression errors of different pruning techniques (magnitude, singular value, or node pruning) become arbitrarily small as the network size increases. We further prove generalization bounds adapted to our theoretical framework, which are consistent with the observation that the generalization error will be lower for more compressible networks. Our theory and numerical study on various neural networks show that large step-size/batch-size ratios introduce heavy tails, which, in combination with overparametrization, result in compressibility.

1 Introduction

With the increasing model sizes in deep learning and with its increasing use in low-resource environments, network compression is becoming ever more important. Among many network compression techniques, network pruning has been arguably the most commonly used method [O'N20], and it is rising in popularity and success [BOFG20]. Though various pruning methods are successfully used in practice and their theoretical implications in terms of generalization are increasingly apparent [AGNZ18], a thorough understanding of *why* and *when* neural networks are compressible is lacking.

*Equal contribution.

A common conclusion in pruning research is that overparametrized networks can be greatly compressed by pruning with little to no cost at generalization, including with simple schemes such as magnitude pruning [BOFG20, O’N20]. For example, research on *iterative magnitude pruning* [FC19] demonstrated the possibility of compressing trained deep learning models by iteratively eliciting a much sparser substructure. While it is known that the choice of training hyperparameters such as learning rate affects the performance of such pruning strategies [FDRC20, HJRY20, RFC20], usually such observations are low in granularity and almost never theoretically motivated. Overall, the field lacks a framework to understand why or when a pruning method should be useful [O’N20].

Another strand of research that highlights the importance of understanding network compressibility includes various studies [AGNZ18, SAM⁺20, SAN20, HJTW21, KLG⁺21] that presented generalization bounds and/or empirical evidence that imply that the more compressible a network is, the more likely it is to generalize well. The aforementioned bounds are particularly interesting since classical generalization bounds increase with the dimension and hence become irrelevant in high dimensional deep learning settings, and fall short of explaining the generalization behavior of overparametrized neural networks. These results again illustrate the importance of understanding the conditions that give rise to compressibility given their implications regarding generalization.

In this paper, we develop a theoretical framework to address (i) *why and when modern neural networks can be amenable to very simple pruning strategies* and (ii) *how this relates to generalization*. Our theoretical results are based on two recent disparate discoveries regarding deep neural networks trained with the stochastic gradient descent (SGD) algorithm. The first one is the emergence of *heavy-tailed* stationary distributions, which appear when the networks are trained with large learning rates and/or small batch-sizes [HM20, GSZ21]. The second one is the *propagation of chaos* phenomenon, which indicates that, as the network size goes to infinity, the network weights behave *independently* [MMN18, SS20, DBDF20].

We show that, assuming both of the aforementioned phenomena occur *simultaneously*, fully connected neural networks will be provably compressible in a precise sense, and the compression errors of (i) unstructured global or layer-wise magnitude pruning, (ii) pruning based on singular values of the weight matrices, (iii) and node pruning can be made arbitrarily small for any compression ratio as the dimension increases. Our formulation of network compressibility in terms of ‘ ℓ_p -compressibility’ enables us to access results from *compressed sensing* literature [GCD12, AUM11] to be used in neural network analysis. Moreover, we prove generalization bounds adapted to our framework that agree with existing compression-based generalization bounds [AGNZ18, SAM⁺20, SAN20] and confirm that compressibility implies better generalization. We conduct experiments on fully connected and convolutional networks and show that the results are in strong accordance with our theory.

Our study reveals an interesting phenomenon: depending on the algorithm hyperparameters, such as learning rate and batch-size, the resulting neural networks might possess different compressibility properties. Under the decoupling effect of propagation of chaos that emerges with overparametrization [DBDF20], the networks become compressible in a way that they are amenable to simple pruning strategies as the tails get heavier, which is shown to depend on the step-size/batch-size ratio [GSZ21]. Finally, when compressible, the networks become likely to generalize better. In this sense, our results also provide an alternative perspective to the recent theoretical studies that suggest that heavy tails can be beneficial in terms of generalization [SSDE20, ZFM⁺20].

2 Preliminaries and Technical Background

Notation. Matrices and vectors are denoted by upper- and lower-case bold letters, respectively, e.g. \mathbf{X} and \mathbf{x} . A sequence of n scalars x_1, \dots, x_n is shown as $\{x_i\}_{i=1}^n$. Similar notations are used for sequences of matrices $\{\mathbf{X}_i\}_{i=1}^l$ and vectors $\{\mathbf{x}_i\}_{i=1}^l$, whose entries are indexed with convention $\mathbf{X}_i = [\mathbf{X}_i]_{m,n}$ and $\mathbf{x}_i = (x_{i,1}, x_{i,2}, \dots, x_{i,n})$, respectively. The set of integers $\{m, \dots, n\}$ is denoted by $\llbracket m, n \rrbracket$. We denote the ℓ_p (semi-)norm of a vector $\mathbf{x} \in \mathbb{R}^d$ as $\|\mathbf{x}\|_p = (\sum_{i=1}^d |x_i|^p)^{1/p}$ for all $p \in (0, \infty)$ and $\|\mathbf{x}\|$ implies $\|\mathbf{x}\|_2$. For a matrix $\mathbf{A} \in \mathbb{R}^{n \times m}$, $\|\mathbf{A}\|$ denotes its Frobenius norm.

Fully connected neural networks. In the entirety of the paper, we consider a multi-class classification setting. We denote the space of data points by $\mathcal{Z} = \mathcal{X} \times \mathcal{Y}$, where $\mathcal{X} \subset \mathbb{R}^{d_x}$ is the space of features and $\mathcal{Y} = \{1, 2, \dots, d_Y\}$ is the space of the labels. Similar to prior art (e.g., [NBS18]), we focus our attention on the bounded feature domain $\mathcal{X} = \mathcal{X}_B := \{\mathbf{x} \in \mathbb{R}^{d_x}; \|\mathbf{x}\| \leq B\}$.

We denote a *fully connected neural network* with L layers by a collection of *weight matrices* $\{\mathbf{W}_l\}_{l=1}^L$, such that $\mathbf{W}_l \in \mathbb{R}^{h_l \times h_{l-1}}$, where h_l denotes the number of hidden units at layer l with $h_0 = d_X$ and $h_L = d_Y$. Accordingly, the *prediction function* $f_{\mathbf{w}}(\mathbf{x}) : \mathcal{X}_B \mapsto \mathbb{R}^{d_Y}$, with elements $f_{\mathbf{w}}(\mathbf{x}) := (f_{\mathbf{w}}(\mathbf{x})[1], \dots, f_{\mathbf{w}}(\mathbf{x})[d_Y])$, corresponding to the neural network is defined as follows:

$$f_{\mathbf{w}}(\mathbf{x}) = \mathbf{W}_L \phi(\mathbf{W}_{L-1} \phi(\dots \phi(\mathbf{W}_1 \mathbf{x}))), \quad (1)$$

where $\phi : \mathbb{R} \rightarrow \mathbb{R}$ is the rectified linear unit (ReLU) activation function, i.e., $\phi(x) = \max(0, x)$, and it is applied element-wise when its input is a vector. For notational convenience, let us define $d_l := h_l \times h_{l-1}$ and $d := \sum_{l=1}^L d_l$. Furthermore, let \mathbf{w}_l denote the *vectorized* weight matrix of layer l , i.e., $\mathbf{w}_l := \text{vec}(\mathbf{W}_l) \in \mathbb{R}^{d_l}$, where **vec** denotes vectorization. Finally, let \mathbf{w} be the concatenation of all the vectorized weight matrices, i.e., $\mathbf{w} := [\mathbf{w}_1, \dots, \mathbf{w}_L] \in \mathbb{R}^d$. We assume that $L \geq 2$.

Risk minimization and SGD. In order to assess the quality of a neural network represented by its weights \mathbf{w} , we consider a loss function $\ell : \mathcal{Y} \times \mathcal{Y} \mapsto \mathbb{R}_+$, such that $\ell(y, f_{\mathbf{w}}(\mathbf{x}))$ measures the loss incurred by predicting the label of \mathbf{x} as $\arg \max_j f_{\mathbf{w}}(\mathbf{x})[j]$, when the true label is y . By following a standard statistical learning theoretical setup, we consider an unknown *data distribution* μ_Z over \mathcal{Z} , and a *training dataset* with n elements, i.e., $S = \{\mathbf{z}_1, \dots, \mathbf{z}_n\}$, where each $\mathbf{z}_i =: (\mathbf{x}_i, y_i) \stackrel{\text{i.i.d.}}{\sim} \mu_Z$. We then denote the *population* and *empirical risks* as $\mathcal{R}(\mathbf{w}) := \mathbb{E}_{(\mathbf{x}, y) \sim \mu_Z} [\ell(y, f_{\mathbf{w}}(\mathbf{x}))]$ and $\widehat{\mathcal{R}}(\mathbf{w}) := \frac{1}{n} \sum_{i=1}^n \ell(y_i, f_{\mathbf{w}}(\mathbf{x}_i))$.

Since μ_Z is unknown, we cannot directly attempt to minimize \mathcal{R} in practice. One popular approach to address this problem is the *empirical risk minimization* strategy, where the goal is to solve the following optimization problem: $\min_{\mathbf{w} \in \mathbb{R}^d} \widehat{\mathcal{R}}(\mathbf{w})$. To tackle this problem, SGD has been one of the most popular optimization algorithms, which is based on the following simple recursion:

$$\mathbf{w}^{\{k+1\}} = \mathbf{w}^{\{k\}} - \eta \nabla \widetilde{\mathcal{R}}_{k+1}(\mathbf{w}^{\{k\}}), \quad \text{where } \nabla \widetilde{\mathcal{R}}_k(\mathbf{w}) := (1/b) \sum_{i \in \Omega_k} \nabla \ell(y_i, f_{\mathbf{w}}(\mathbf{x}_i)). \quad (2)$$

Here, $\mathbf{w}^{\{k\}}$ denotes the weight vector at iteration $k \in \mathbb{N}^+$, $\eta > 0$ is the step-size (or learning rate), $\nabla \widetilde{\mathcal{R}}_k(\cdot)$ is the stochastic gradient, and Ω_k is the mini-batch with size b , drawn with or without replacement from $\llbracket 1, n \rrbracket$.

Heavy-tailed distributions and the α -stable family. In this study, we will mainly deal with heavy-tailed random variables. While there exist different definitions of heavy tails in the literature, here, we call a random variable heavy-tailed if its distribution function has a *power-law* decay, i.e., $\mathbb{P}(X \geq x) \sim cx^{-\alpha}$ as $x \rightarrow \infty$, for some $c > 0$ and $\alpha \in (0, 2)$. Here, the *tail index* α determines the tail thickness of the distribution, i.e., as α get smaller, the distribution becomes heavier-tailed.

An important subclass of heavy-tailed distributions is the family of stable distributions. A random variable X has symmetric α -stable distribution, denoted by $\mathcal{S}\alpha\mathcal{S}(\sigma)$, if its characteristic function is equal to $\mathbb{E}[\exp(iwX)] = \exp(-|\sigma w|^\alpha)$, where $\alpha \in (0, 2]$ is again the tail index and $\sigma \in (0, \infty)$ is the scale parameter. An important property of $\mathcal{S}\alpha\mathcal{S}$ is that whenever $\alpha < 2$, $\mathbb{E}|X|^p$ is finite if and only if $p < \alpha$. This implies that the distribution has infinite variance as soon as $\alpha < 2$. In addition to their wide use in applied fields [Nol20], recently, $\mathcal{S}\alpha\mathcal{S}$ distributions have also been considered in deep learning theory [SSG19, PFF20, ZFM⁺20, §SDE20] and optimization [WGZ⁺21].

3 Compressibility and the Heavy-Tailed Mean-Field Regime

In this section, we will present our first set of theoretical results. We first identify a sufficient condition, then we prove that, under this condition, the compression errors of different pruning techniques become arbitrarily small as the network size increases.

3.1 The heavy-tailed mean-field regime

Due to the peculiar generalization behavior of neural networks trained with SGD, recent years have witnessed an extensive investigation of the theoretical properties of SGD in deep learning [Lon17, DR17, KL18, ZZL19, AZLL19, §SDE20, Neu21, CDE⁺21, BLG§21]. We will now mention two recently established theoretical properties of SGD, and our main contribution is studying the compressibility properties of the network under the assumption that these two seemingly unrelated ‘phenomena’ occur simultaneously.

The heavy tail phenomenon. Several recent studies [MM19, SSG19, §GN⁺19, §ZTG20, ZFM⁺20, ZKV⁺20, CWZ⁺21] have empirically illustrated that neural networks can exhibit heavy-tailed

behavior when optimized with SGD. Theoretically investigating the origins of this heavy-tailed behavior, [HM20] and [GSZ21] later proved several theoretical results on online SGD, with rather surprising implications: due to the ‘multiplicative’ structure of the gradient noise (*i.e.*, $\nabla \hat{\mathcal{R}}_k(\mathbf{w}) - \nabla \hat{\mathcal{R}}(\mathbf{w})$), as $k \rightarrow \infty$, the distribution of the SGD iterates $\mathbf{w}^{\{k\}}$ can converge to a heavy-tailed distribution with *infinite second-order moment*, and perhaps more surprisingly, this behavior can even emerge in simple linear regression with Gaussian data. The authors of [GSZ21] further showed that, in the linear regression setting, the tail index α is *monotonic* with respect to the step-size η and batch-size b : larger η and/or smaller b result in smaller α (*i.e.*, heavier tails).

Propagation of chaos and mean-field limits. Another interesting property of SGD appears when the size of the network goes to infinity. Recently, it has been shown that, under an appropriate scaling of step-sizes, the empirical distribution of the network weights converges to a fixed *mean-field* distribution, and the SGD dynamics can be represented as a *gradient flow* in the space of probability measures [MMN18, CB18, SS20, DBDF20]. Moreover, [DBDF20] showed that a *propagation of chaos* phenomenon occurs in this setting, which indicates that when the network weights are initialized independently (*i.e.*, a-priori chaotic behavior), *the weights stay independent* as the algorithm evolves over time (*i.e.*, the chaos propagates) [Szn91].

Our focus in this paper is the setting where both of these phenomena occur *simultaneously*: we assume that as the size of the network goes to infinity, the SGD iterates become *independent* and their distribution converges to a *heavy-tailed* distribution. To formalize this setting, let us introduce the required notations. For an integer $m_l < d_l$, let $\mathbf{w}_{l,(1:m_l)}$ denote the first m_l coordinates of \mathbf{w}_l , and for $m_l \geq d_l$ set $\mathbf{w}_{l,(1:m_l)} = \mathbf{w}_l$. Furthermore, parametrize the dimension of each layer d_l with a parameter $\rho \in \mathbb{R}$, *i.e.*, $d_l = d_l(\rho)$, such that for all $l = 1, \dots, L$, we have:

$$d_l(\rho) \in \mathbb{N}_+, \quad \text{and} \quad \lim_{\rho \rightarrow \infty} d_l(\rho) = \infty. \quad (3)$$

This construction enables us to take the dimensions of each layer to infinity simultaneously [NP21].

Condition 1 (Heavy-tailed mean-field limit condition). *The SGD recursion (2) satisfies the heavy-tailed mean-field limit (HML) condition, if the dimensions obey (3) and if there exist heavy-tailed probability measures $\{\mu_l^*\}_{l=1}^L$ on \mathbb{R} with tail indices $\{\alpha_l\}_{l=1}^L$, such that $\mu_l^*(\{0\}) = 0$ for all l and for any $m_1, \dots, m_L \in \mathbb{N}_+$, the joint distribution of*

$$\left(\mathbf{w}_{1,(1:m_1)}^{\{k\}}, \dots, \mathbf{w}_{L,(1:m_L)}^{\{k\}} \right) \quad \text{weakly converges to} \quad (\mu_1^*)^{\otimes m_1} \otimes \dots \otimes (\mu_L^*)^{\otimes m_L}, \quad (4)$$

as $\rho, k \rightarrow \infty$, where $\mu \otimes \nu$ denotes the product measure and $\mu^{\otimes n}$ denotes the n -fold product measure.

Informally, the HML condition states that in the infinite size and infinite iteration limit, the entries of the weight matrices will become independent, and the distribution of the elements within the same layer will be identical and heavy-tailed. We acknowledge that the above condition may not be always satisfied, and theoretical evidence for this condition is provided in rather seemingly simpler settings such as linear regression [GSZ21] and/or two-layer neural networks [DBDF20]. However, we will empirically illustrate the behavior described by the HML condition in Section 5 in certain scenarios. Note that, in (4), the particular form of independence in the limit is not crucial and we will discuss weaker alternatives in Section 3.3.

We further note that [DBDF20] proved that a similar form of (4) indeed holds for SGD applied on single hidden-layered neural networks, where the limiting distributions possess second-order moments (*i.e.*, not heavy-tailed) and the independence is column-wise. Recently, [PFF20] investigated the infinite width limits of fully connected networks initialized from a $\mathcal{S}\alpha\mathcal{S}$ distribution and proved heavy-tailed limiting distributions. On the other hand, heavy-tailed propagation of chaos results have been proven in theoretical probability [JMW08, LMW20]; however, their connection to SGD has not been yet established. We believe that (4) can be shown to hold under appropriate conditions, which we leave as future work.

3.2 Analysis of compression algorithms

In this section, we will analyze the compression errors of three different compression schemes under the HML condition. All three methods are based on *pruning*, which we formally define as follows. Let \mathbf{x} be a vector of length d , and consider its sorted version in descending order with respect to the magnitude of its entries, *i.e.*, $|x_{i_1}| \geq |x_{i_2}| \geq \dots \geq |x_{i_d}|$, where $\{i_1, \dots, i_d\} = \{1, \dots, d\}$. For any $k \leq d$, the k -best term approximation of \mathbf{x} , denoted as $\mathbf{x}^{(k)} = (x_1^{(k)}, \dots, x_d^{(k)})$, is defined as follows:

for $l \in \llbracket 1, \lceil k \rceil \rrbracket$, $x_{i_l}^{(k)} := x_{i_l}$ and for $l \notin \llbracket 1, \lceil k \rceil \rrbracket$, $x_{i_l}^{(k)} := 0$. Informally, we keep the k -largest entries of \mathbf{x} with the largest magnitudes, and ‘prune’ the remaining ones. Current results pertain to one-shot pruning with no fine-tuning; other settings are left for future work (cf. [EKT20]).

In this section, we consider that we have access to a sample from the stationary distribution of the SGD, *i.e.* $\mathbf{w}^{\{\infty\}}$, and for conciseness we will simply denote it by \mathbf{w} . We then consider a *compressed network* $\hat{\mathbf{w}}$ (that can be obtained by different compression schemes) and measure the performance of the compression scheme by its ‘relative ℓ_p -compression error’ (cf. [AUM11, GCD12]), defined as: $\|\hat{\mathbf{w}} - \mathbf{w}\|_p / \|\mathbf{w}\|_p$. Importantly for the following results, in the supplement, we further prove that a small compression error also implies a small perturbation on the network output.

Magnitude pruning. Magnitude pruning has been one of the most common and efficient algorithms among all the network pruning strategies [HPTD15, BOFG20, KLG⁺21]. In this section, we consider the global and layer-wise magnitude pruning strategies under the HML condition.

More precisely, given a network weight vector $\mathbf{w} \in \mathbb{R}^d$ and a *remaining parameter ratio* $\kappa \in (0, 1)$, the global pruning strategy compresses \mathbf{w} by using $\mathbf{w}^{(\kappa d)}$, *i.e.*, it prunes the smallest (in magnitude) $(1 - \kappa)d$ entries of \mathbf{w} . Also, note that $1/\kappa$ corresponds to the frequently used metric *compression rate* [BOFG20]. On the other hand, the layer-wise pruning strategy applies the same approach to each layer separately, *i.e.*, given layer-wise remaining parameter ratios $\kappa_l \in (0, 1)$, we compress each layer weight $\mathbf{w}_l \in \mathbb{R}^{d_l}$ by using $\mathbf{w}_l^{(\kappa_l d_l)}$. The following result shows that the compression error of magnitude pruning can be made arbitrarily small as the network size grows.

Theorem 1. *Assume that the recursion (2) satisfies the HML condition.*

- (i) *Global magnitude pruning: if the weights of all layers have identical asymptotic distributions $\mu_l^* \equiv \mu^*$ with tail index $\alpha_l^* = \alpha$, for all $l \in \llbracket 1, L \rrbracket$, then for every $\epsilon > 0$, $\epsilon_l > 0$, $\kappa \in (0, 1)$, and $p \geq \alpha$, there exists $d_0 \in \mathbb{N}$, such that $\|\mathbf{w}^{(\kappa d)} - \mathbf{w}\|_p \leq \epsilon \|\mathbf{w}\|_p$ holds with probability at least $1 - \epsilon$, for $d \geq d_0$.*
- (ii) *Layer-wise magnitude pruning: for every $\epsilon > 0$, $\epsilon_l > 0$ and $\kappa_l \in (0, 1)$, where $l \in \llbracket 1, L \rrbracket$, and $p \geq \max_l \alpha_l$, there exists $d_{l,0} \in \mathbb{N}$, such that $\|\mathbf{w}_l^{(\kappa_l d_l)} - \mathbf{w}_l\|_p \leq \epsilon_l \|\mathbf{w}_l\|_p$ holds with probability at least $1 - \epsilon$, for $d_l \geq d_{l,0}$.*

This result shows that any pruning ratio of the weights is achievable as long as the network size is sufficiently large and the network weights are close enough to an i.i.d. heavy-tailed distribution. Empirical studies report that global magnitude pruning often works better than layer-wise magnitude pruning [BOFG20], except when it leads to over-aggressive pruning of particular layers [WZG20].

The success of this strategy under the HML condition is due to a result from compressed sensing theory, concurrently proven in [GCD12, AUM11], which informally states that for a large vector of i.i.d. heavy-tailed random variables, the norm of the vector is mainly determined by a small fraction of its entries. We also illustrate this visually in the supplementary document.

An important question here is that, to achieve a fixed relative error ϵ_l , how would the smallest κ_l differ with varying tail-indices α_l , *i.e.*, whether ‘‘heavier tails imply more compression’’. In our experiments, we illustrate this behavior positively: heavier-tailed weights are indeed more compressible. We partly justify this behavior for a certain range of p in the supplement; however, a more comprehensive theory is needed, which we leave as future work.

Singular value pruning. In recent studies, it has been illustrated that the magnitudes of the eigenvalues of the sample covariance matrices (for different layers) can decay quickly, hence pruning the singular values of the weight matrices, *i.e.*, only keeping the largest singular values and corresponding singular vectors, is a sensible pruning method. Exploiting the low-rank nature of fully connected and convolutional layer weights in network compression has been investigated theoretically and empirically [AGNZ18, YLWT17]. Here we will present a simple scheme to demonstrate our results.

More precisely, for the weight matrix at layer l , \mathbf{W}_l , consider its singular value decomposition, $\mathbf{W}_l = \mathbf{U}\Sigma\mathbf{V}^\top$, and then, with a slight abuse of notation, define $\mathbf{W}_l^{[\kappa_l h_{l-1}]} := \mathbf{U}\Sigma^{(\kappa_l h_{l-1})}\mathbf{V}^\top$, where $\Sigma^{(\kappa_l h_{l-1})}$ is the diagonal matrix whose diagonal entries contain the $\lceil \kappa_l h_{l-1} \rceil$ largest singular values (*i.e.*, prune the diagonal of Σ). Accordingly, denote $\mathbf{w}_l^{[\kappa_l h_{l-1}]} := \text{vec}(\mathbf{W}_l^{[\kappa_l h_{l-1}]})$.

The next theorem shows that under the HML condition with an additional requirement that the limiting distributions are $\mathcal{S}\alpha\mathcal{S}$, the eigenvalues of the (properly normalized) sample covariance matrices will be indeed compressible and the pruning strategy achieves negligible errors as the network size grows.

Theorem 2. *Assume that the recursion (2) satisfies the HML condition, $L \geq 3$, and for all $l \in \llbracket 2, L-1 \rrbracket$, $\mu_l^* \equiv \mathcal{S}\alpha_l\mathcal{S}(\sigma_l)$ with some $\sigma_l > 0$. Then, for every $\epsilon > 0$, $\varepsilon_l > 0$, and $\kappa_l \in (0, 1)$, there exists $\{h_{l,0}\}_{l=1}^L$, such that the following inequalities hold for every $h_l \geq h_{l,0}$ and $p \geq \max_l \alpha_l/2$:*

$$\|\lambda_l^{(\kappa_l h_{l-1})} - \lambda_l\|_p \leq \varepsilon_l^2 \|\lambda_l\|_p, \quad \text{and} \quad \|\mathbf{w}_l^{[\kappa_l h_{l-1}]} - \mathbf{w}_l\| \leq \varepsilon_l \|\mathbf{w}_l\|, \quad (5)$$

with probability at least $1 - \epsilon$, where $\lambda_l \in \mathbb{R}^{h_{l-1}}$ denotes the vector of eigenvalues corresponding to the sample covariance matrix $h_l^{-2/\alpha_l} \mathbf{W}_l^\top \mathbf{W}_l$.

We shall note that the proof of Theorem 2 in fact only requires the limiting distributions to be ‘regularly varying’ [TTR⁺20] and symmetric around zero, which covers a broad range of heavy-tailed distributions beyond the α -stable family [BDM⁺16]. The sole reason why we require the $\mathcal{S}\alpha\mathcal{S}$ condition here is to avoid introducing further technical notation.

In Theorem 2, p needs to be greater than or equal to $\alpha/2$, in contrast to the condition $p \geq \alpha$ in Theorem 1. The reason is that Theorem 2 is based on pruning the eigenvalues of the normalized covariance matrix and moreover in general if a matrix $\mathbf{A} \in \mathbb{R}^{n \times m}$ has elements $[\mathbf{A}]_{i,j}$ that are independent and identically distributed from the symmetric α -stable distribution, then by [TTR⁺20, Theorem 2.7], as $m \rightarrow \infty$, the eigenvalues of $m^{-2/\alpha} \mathbf{A}^T \mathbf{A}$ weakly converge to independent random variables, that are identically distributed from a positive stable distribution with tail index $\alpha/2$.

Node pruning. The last pruning strategy that we consider is a structured pruning strategy, that corresponds to the removal of the whole columns of a fully connected layer weight matrix. Even though below we consider pruning based on the norms of the weight layer columns, the same arguments apply for pruning rows; see supplement for further discussion.

The idea in column pruning is that, for a given layer l , we first sort the columns of the weight matrix $\mathbf{W}_l \in \mathbb{R}^{h_l \times h_{l-1}}$ with respect to their ℓ_p -norms for a given $p \geq \max_l \alpha_l$. Then, we remove the *entire columns* that have the smallest ℓ_p -norms. More precisely, let $\mathbf{W}_l(i) \in \mathbb{R}^{h_l}$ be the i -th column of \mathbf{W}_l , for $i \in \llbracket 1, h_{l-1} \rrbracket$, and suppose that $\|\mathbf{W}_l(i_1)\|_p \geq \|\mathbf{W}_l(i_2)\|_p \geq \dots \geq \|\mathbf{W}_l(i_{h_{l-1}})\|_p$, where $\{i_1, \dots, i_{h_{l-1}}\} = \{1, \dots, h_{l-1}\}$. Then, we define the k -best column approximation of \mathbf{W}_l , denoted as $\mathbf{W}_l^{\{k\},p} \in \mathbb{R}^{h_l \times h_{l-1}}$, as follows: for $j \in \llbracket 1, \lceil k \rceil \rrbracket$, $\mathbf{W}_l^{\{k\},p}(i_j) := \mathbf{W}_l(i_j)$ and for $j \notin \llbracket 1, \lceil k \rceil \rrbracket$, $\mathbf{W}_l^{\{k\},p}(i_j) := 0$. Denote also $\mathbf{w}_l^{\{k\},p} := \text{vec}(\mathbf{W}_l^{\{k\},p})$.

Theorem 3. *Assume that the recursion (2) satisfies the HML condition. Then, for every $\epsilon > 0$, $\varepsilon_l > 0$, $\kappa_l \in (0, 1)$, where $l \in \llbracket 2, L \rrbracket$, and $p \geq \max_l \alpha_l$, there exists $h_{l-1,0} \in \mathbb{N}$, such that $\|\mathbf{w}_l^{\{\kappa_l h_{l-1}\},p} - \mathbf{w}_l\|_p \leq \varepsilon_l \|\mathbf{w}_l\|_p$ holds with probability at least $1 - \epsilon$, for every $h_{l-1} \geq h_{l-1,0}$.*

This theorem indicates that we can remove entire columns in each layer, without considerably affecting the network weights, as long as the network is large enough. In other words, effectively the widths of the layers can be reduced. Structured pruning schemes are commonly used in CNNs where filters, channels, or kernels can be pruned by norm-based or other criteria [LKD⁺17, HZS17, HPTD15].

3.3 A note on the limiting independence structure in the HML condition

We conclude this section by discussing the particular independence condition in the limit, which appears in Condition 1. We shall underline that the element-wise independence is not a necessity and under weaker conditions, we can still obtain Theorems 1-3 with identical or almost identical proofs. For instance, the proof of Theorem 3 remains the same when the columns of \mathbf{W}_l are i.i.d. vectors with *dependent* components; hence, the element-wise independence is indeed not needed, but is used for the clarity of presentation. More generally, in all three theorems, the main requirement is to ensure a *weak dependence* between the components of the weight vector. More precisely, for Theorems 1, 2, 3, we respectively need (1) the entries of \mathbf{W}_l or (2) its singular values, or (3) the ℓ_p -norms of its columns to be *stationary* and *ergodic* with a heavy-tailed distribution. Under this condition, the same proof strategies will still work by invoking [SD15, Theorem 1], instead of [GCD12, Proposition 1].

4 Generalization Bounds

So far, we have shown that the heavy-tailed behavior in the weights of a network together with their independence result in compressibility. In this section, we further show that these phenomena bring forth a better generalization performance bound in the network. More precisely, we establish a generalization bound such that if a network is more compressible, then the corresponding compressed network has a smaller generalization error bound. Throughout the section, we will focus on layer-wise magnitude pruning; yet, our results can be easily extended to the other pruning strategies. Note that similar results have already been proven in [AGNZ18, SAM⁺20, SAN20, HJTW21]; yet, they cannot be directly used in our specific setting, hence, we prove results that are customized to our setup. More precisely, although these works, similar to our result, are based on the assumption of the “compressibility” of the network and moreover the generalization gap of the population risk with respect to the empirical margin risk is considered in [AGNZ18, HJTW21], they cannot be applied directly to the ℓ_p -compressibility based strategies discussed in the previous section. We should emphasize that our results, as well as the previous mentioned works, are merely *upper bounds* on the generalization performance of the network.

Our generalization bounds are derived by applying the previously developed techniques as in [AGNZ18, NBS18]. In particular, we follow the approach of [AGNZ18] by further adapting the technique for the magnitude pruning strategy and allowing the compressed network weights to take unbounded continuous values. As in [AGNZ18], we consider the 0-1 loss function with *margin* $\gamma \geq 0$, $\ell_\gamma: \mathcal{Y} \times \mathcal{Y} \mapsto \{0, 1\}$, for the multiclass classifier $f_{\mathbf{w}}$, given as follows:

$$\ell_\gamma(y, f_{\mathbf{w}}(\mathbf{x})) = \begin{cases} 1, & \text{if } f_{\mathbf{w}}(\mathbf{x})[y] - \max_{j \neq y} f_{\mathbf{w}}(\mathbf{x})[j] \leq \gamma, \\ 0, & \text{otherwise.} \end{cases} \quad (6)$$

Still denoting $\mathbf{w} = \mathbf{w}^{\{\infty\}}$, the population and empirical risks associated with ℓ_γ are denoted as $\mathcal{R}_\gamma(\mathbf{w})$ and $\widehat{\mathcal{R}}_\gamma(\mathbf{w})$, respectively. By having the dataset $S \sim \mu_Z^{\otimes n}$, we assume the weights \mathbf{w} are sampled according to the stationary distribution $P_{\mathbf{w}|S}$ of SGD. Denote the joint distribution of (S, \mathbf{w}) by $P_{S, \mathbf{w}} := \mu_Z^{\otimes n} P_{\mathbf{w}|S}$.

In the following theoretical results, we will assume that we have access to a random compressible neural network that is amenable to the layer-wise magnitude pruning strategy with high probability. This assumption is essentially the outcome of Theorem 1 under the HML condition together with an additional uniformity requirement on $d_{l,0}$ over S^1 .

H 1. For $\varepsilon \geq 0$, $\epsilon > 0$, and $\{\kappa_l\}_{l=1}^L: \kappa_l \in (0, 1)$, there exists $\{d_{l,0}\}_{l=1}^L: d_{l,0} \in \mathbb{N}$ independent of S , such that for $d_l \geq d_{l,0}$, $l \in \llbracket 1, L \rrbracket$, the relation $\|\widehat{\mathbf{w}}_l - \mathbf{w}_l\| \leq \varepsilon \|\mathbf{w}_l\|$ holds for all $l \in \llbracket 1, L \rrbracket$ simultaneously with probability at least $1 - \epsilon$, where $\widehat{\mathbf{w}}_l := \mathbf{w}_l^{(\kappa_l d_l)}$ and the probability is w.r.t. $P_{S, \mathbf{w}}$.

In the following result, we relate the population risk of the compressed network to the empirical margin risk of the original (uncompressed) network. For notational convenience, for $\delta, \tau > 0$, let

$$R(\delta) := \inf\{R: \mathbb{P}(\|\mathbf{w}\| \geq R) \leq \delta\}, \text{ and } \mathcal{L}(\tau, \delta) := \sqrt{2}BL \left(2R(\delta)/\sqrt{L}\right)^{L-1}/\tau, \quad (7)$$

where the probability is with respect to the joint distribution $P_{S, \mathbf{w}}$.

Theorem 4. Assume **H 1** holds. Then for $n: n/\log(n) \geq 10L$, $\{d_l\}_{l=1}^L: d_l \geq d_{l,0}$, and any $\delta, \tau > 0$, with probability at least $1 - 2e^{-\kappa d/2} - \delta - \epsilon$,

$$\mathcal{R}_0(\widehat{\mathbf{w}}) \leq \widehat{\mathcal{R}}_{\gamma(\delta, \tau)}(\mathbf{w}) + \left(12\mathcal{L}(\tau, \delta)R(\delta) + \sqrt{d}\right) \sqrt{(\kappa + \epsilon_\kappa) \log(n)/n}, \quad (8)$$

where $R(\delta)$ and $\mathcal{L}(\tau, \delta)$ are defined in (7), $\kappa := \frac{1}{d} \sum_{l=1}^L \lceil \kappa_l d_l \rceil$,²

$$\epsilon_\kappa := (2h_b(\kappa) - \kappa \log(\kappa))/\log(n), \text{ and } \gamma(\delta, \tau) := \tau + \frac{\sqrt{2}B}{\tau} \left(R(\delta)/\sqrt{L}\right)^L ((1 + \varepsilon)^L - 1).$$

¹Note that the uniformity assumption is mild and can be avoided by combining Theorem 1 with Egoroff’s theorem with additional effort, as in [SSDE20].

²The binary entropy $h_b(\kappa)$ (in nats) is defined as $-\kappa \log(\kappa) - (1 - \kappa) \log(1 - \kappa)$ for $\kappa \in [0, 1]$, with the convention $h_b(0) = h_b(1) = 0$. Note that $0 \leq h_b(\kappa) \leq \log(2)$.

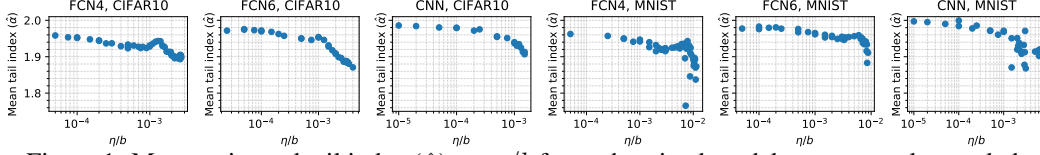


Figure 1: Mean estimated tail index ($\hat{\alpha}$) vs. η/b for each trained model. x -axes are log-scaled.

This result establishes a generalization bound such that, for a fixed relative compression error ε , if a network is more compressible, *i.e.* if κ is smaller, then its corresponding compressed network has a smaller generalization error bound, as the bound is scaled by the factor $\approx \sqrt{\kappa}$.

In our proof, we prove an intermediate result, inspired by [NTS15] and stated in the supplement, which bounds the perturbation of the network output after compression. This guarantees that the risks of the original and pruned networks can be made arbitrarily close, as long as the relative compression error is small enough.

To have a better understanding of the constants in Theorem 4, in the next result, we consider a special case where the weights follow a stable distribution, and we make the above bound more explicit.

Corollary 1. Assume that for $l \in \llbracket 1, L \rrbracket$ and $i \in \llbracket 1, d_l \rrbracket$, the conditional distribution of $w_{l,i} \stackrel{i.i.d.}{\sim} S_{\alpha_l} S(\sigma_l)$ with $\alpha_l \in (1, 2)$. Further, assume that the scale parameters satisfy the following property:

$$\sigma^2 := \sum_{l=1}^L (d_l/d) (\sigma_l/\sigma_{\alpha_l})^2 = \left[(4^{-1/\alpha} \sqrt{L}/3) \sigma_0 d^{-(1/2+1/\alpha)} \right]^2, \quad (9)$$

where $\sigma_{\alpha_l} := (2\Gamma(-\alpha_l) \cos((2-\alpha_l)\pi/2))^{1/\alpha_l}$, $\alpha := \min_l \alpha_l$, and σ_0 is a constant, and also $\{\alpha_l\}_{l=1}^L$ and σ are independent from S . Then, for every $\varepsilon > 0$ and $\kappa_l \in (0, 1)$, $l \in \llbracket 1, L \rrbracket$, there exists $d_{l,0} \in \mathbb{N}$, such that for $d_l \geq d_{l,0}$, $n: n/\log(n) \geq 10L$, and every $\tau > 0$, with probability at least $1 - 3d^{-\alpha/(2L)}$,

$$\mathcal{R}_0(\hat{\mathbf{w}}) \leq \hat{\mathcal{R}}_\gamma(\mathbf{w}) + (a\sigma_0^L/\tau + 1) \sqrt{(\kappa + \epsilon_\kappa) d \log(n)/n}, \quad (10)$$

where $\{\hat{\mathbf{w}}_1\}_l = \{\mathbf{w}_l^{(\kappa_l d_l)}\}_l$, $\gamma := \tau + b_\varepsilon \sigma_0^L \sqrt{d}/\tau$, $a := 6\sqrt{2}B2^L L^{3/2}$, and $b_\varepsilon := \sqrt{2}B((1+\varepsilon)^L - 1)$.

To simplify our presentation, we have set the ‘scale’ of the distribution as a decreasing function of dimension, which intuitively states that the typical magnitude of each entry of the network will get smaller as the network grows. We observe that for a fixed ε and d , the bound improves as pruning ratio, $1 - \kappa$, increases. This result is of interest in particular since it is observed experimentally (and in part, theoretically) that heavier-tailed weights are more compressible, and hence due to this result have better generalization bounds. This provides an alternative perspective to the recent bounds that aim at linking heavy tails to generalization through a geometric approach [SSDE20].

Finally, in the supplement, we further show that the uncompressed network also inherits this good generalization performance bound, which is consistent with the results of [HJT21, KLG⁺21]: if a network is more ‘compressible’, not only the generalization performance for the compressed network but also for the original network improves. The generalization bound adapted to ℓ_p -compressibility based strategies, discussed in the previous section, is highlighted in Section S2 of the supplement.

5 Experiments

In this section, we present experiments conducted with neural networks to investigate our theory. We use three different model architectures: a fully connected network with 4 hidden layers (FCN4), a fully connected network with 6 hidden layers (FCN6), and a convolutional neural network with 8 convolutional layers (CNN). Hidden layer widths were 2048 for both FCN models. All networks include ReLU activation functions and none include batch normalization, dropout, residual blocks, or any explicit regularization term in the loss function. Each model is trained on MNIST [LCB10] and CIFAR10 [Kri09] datasets under various hyperparameter settings, using the default splits for training and evaluation. The total number of parameters were approximately 14M for FCN4-MNIST, 19M for FCN4-CIFAR10, 23M for FCN6-MNIST, 27M for FCN6-CIFAR10, and 9M for both CNN models. All models were trained with SGD until convergence with constant learning rates and no momentum. The convergence criteria comprised 100% training accuracy and a training negative log-likelihood

less than 5×10^{-5} . The training hyperparameter settings include two batch-sizes ($b = 50, 100$) and various learning rates (η) to generate a large range of η/b values. See the supplement for more details.

By invoking [GŞZ21, Corollary 11] which shows the ergodic average of heavy-tailed SGD iterates converges to a multivariate stable distribution, after convergence, we kept running SGD for 1000 additional iterations to obtain the average of the parameters to be used in this estimation. The tail index estimations were made by the estimator proposed in [MMO15, Corollary 2.4], which has been used by other recent studies that estimate tail index in neural network parameters [ŞSDE20, GŞZ21, ZFM⁺20]. The ergodic averaging does not change the tail index of the parameters, and was employed to facilitate tail index estimation by enabling the utilization of the aforementioned estimator. The rest of the experiments have been conducted without ergodic averaging. We also observe that the results with/without ergodic averaging are virtually identical in both tail index estimation tasks and pruning experiments. In all pruning methods, the parameters were centered before pruning is conducted with the median value to conform with the tail index estimation.

Training hyperparameters and layer statistics. We first verify that models trained with higher learning rate to batch-size ratio (η/b) lead to heavier-tailed parameters, replicating the results presented in [GŞZ21]. For each trained model, we compute the mean of separately estimated tail indices for all layers, so that each model is represented by a single value. This averaging is a heuristic without a clear theoretical meaning, and has been also used by recent works in the literature [GŞZ21, MM19]. Results presented in Figure 1 demonstrates that higher η/b leads to heavier tails (lower $\hat{\alpha}$).

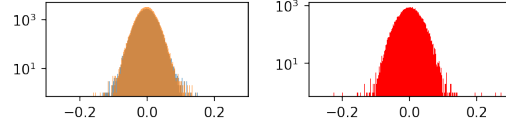


Figure 2: Empirical distribution of a CNN layer trained on MNIST. (Left) Overlaid histograms of a random partition of the weights, showing an identical distribution. (Right) Comparing the network weights to samples simulated i.i.d. from a symmetric α -stable distribution with the same tail index $\alpha \approx 1.95$. y -axes are log-scaled.

Also of interest are the distribution of the resulting parameters from training. Figure 2 (left) demonstrates a representative example of the parameters from an CNN layer trained on MNIST, where two overlaid histograms representing empirical distributions of a random partition of the parameters are almost identical. On the right in the same figure, this distribution is compared to a simulated symmetric α -stable distribution that has the same tail index (≈ 1.95). The figure demonstrates that the two distributions have similar qualitative properties.

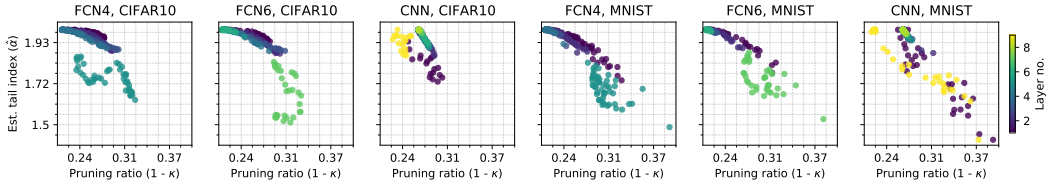


Figure 3: Estimated tail index ($\hat{\alpha}$) vs. pruning ratio ($1 - \kappa$), relative compression error = 0.1, $p = 2$

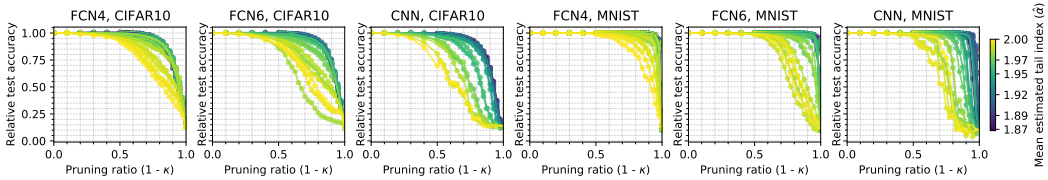


Figure 4: Relative test accuracy vs. pruning ratio for layer-wise magnitude pruning. Colors denote mean estimated tail index ($\hat{\alpha}$).

Tail index and prunability. In this section we examine whether networks with heavier-tailed layers, trained with higher η/b ratios, are more prunable and whether they generalize better. As a baseline test, we first examine whether neural network layers which are heavier-tailed can be pruned more given a fixed maximum relative compression error. Figure 3 demonstrates for an error of 0.1 that this is indeed the case. We next test our hypothesis that posit models with heavy-tailed parameters to be more prunable. Both the results pertaining to layer-wise magnitude pruning and singular value pruning, demonstrated in Figures 4 and 5 show that this is indeed the case. Here, relative test accuracy

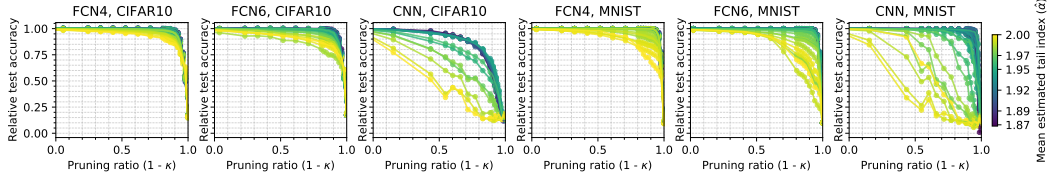


Figure 5: Relative test accuracy vs. pruning ratio for singular value pruning. Colors denote mean estimated tail index ($\hat{\alpha}$).

stands for test accuracy after pruning / unpruned test accuracy. The results show that models with heavier-tailed parameters (shown with darker colors) are starkly more robust against pruning. Similar results with global magnitude pruning can be seen in the supplement.

For structured pruning, we prune 3×3 kernel parameters in CNN models. The results (Figure 6) show a similar, hypothesis conforming pattern. Results for FCNs, presented in the supplement, were underwhelming; perhaps unsurprisingly as structured pruning is not as commonly used in FCNs [O’N20]. More successful attempts could be due to alternative scoring methods [SAM⁺20]; our approach might require wider layers to conform with theoretical conditions.

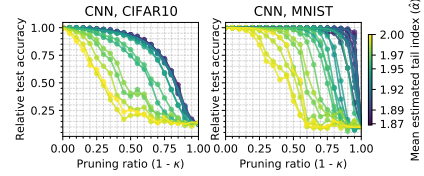


Figure 6: Relative test accuracy vs. pruning ratio for structured pruning. Colors denote mean estimated tail index ($\hat{\alpha}$).

Tail index and generalization. Following our theoretical results, we examine whether the heavier-tailed networks lead to better generalization performance. Consistent with our hypothesis, Figure 7 shows that models with the highest tail index have consistently the worst test performances. The same conclusion applies to generalization performance as training accuracy is 100% for all models. See supplementary material for additional experiment results and discussion of the findings.

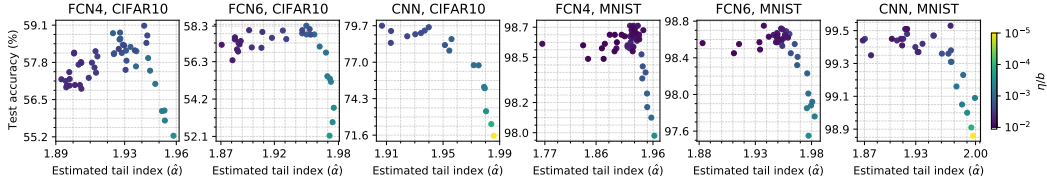


Figure 7: Test accuracy vs. mean estimated tail index ($\hat{\alpha}$) for each model. Color: training η/b ratio.

6 Conclusion

We investigated the conditions under and the mechanism through which various pruning strategies can be expected to work, and confirmed the relationship between pruning and generalization from our theoretical approach. Future directions for research include formally identifying settings in which HML condition holds, eliciting the relationship between $\hat{\alpha}$ and κ more clearly, and further examination of structured pruning in FCNs. Extending our work to other pruning strategies and network structures is also another important future direction. For example, it has recently been observed that gradients also exhibit heavy-tailed behavior [SGN⁺19, ZKV⁺20, ZFM⁺20]; we suspect that our theory might be applicable in the case of gradient-based pruning as well. The extension of our analyses to other network structures such as recurrent layers or ResNet blocks [HZRS15] would also be valuable.

Acknowledgements

The authors are grateful to A. Taylan Cemgil, Valentin De Bortoli, and Mohsen Rezapour for fruitful discussions on various aspects of the paper. MAE is partially funded by CIFAR AI Chairs program, and CIFAR AI Catalyst grant, NSERC Grant [2019-06167]. UŞ’s research is supported by the French government under management of Agence Nationale de la Recherche as part of the “Investissements d’avenir” program, reference ANR-19-P3IA-0001 (PRAIRIE 3IA Institute).

References

- [AGNZ18] Sanjeev Arora, Rong Ge, Behnam Neyshabur, and Yi Zhang. Stronger generalization bounds for deep nets via a compression approach. In *Proceedings of the 35th International Conference on Machine Learning*, volume 80, pages 254–263. PMLR, 10–15 Jul 2018.
- [AUM11] Arash Amini, Michael Unser, and Farokh Marvasti. Compressibility of deterministic and random infinite sequences. *IEEE Transactions on Signal Processing*, 59(11):5193–5201, 2011.
- [AZLL19] Zeyuan Allen-Zhu, Yuanzhi Li, and Yingyu Liang. Learning and generalization in over-parameterized neural networks, going beyond two layers. In H. Wallach, H. Larochelle, A. Beygelzimer, F. d’Alché-Buc, E. Fox, and R. Garnett, editors, *Advances in Neural Information Processing Systems*, volume 32. Curran Associates, Inc., 2019.
- [BDM⁺16] Dariusz Buraczewski, Ewa Damek, Thomas Mikosch, et al. *Stochastic models with power-law tails*. Springer, 2016.
- [Bha97] Rajendra Bhatia. *Matrix Analysis*, volume 169. Springer, 1997.
- [BLGŞ21] Tolga Birdal, Aaron Lou, Leonidas Guibas, and Umut Şimşekli. Intrinsic dimension, persistent homology and generalization in neural networks. In *NeurIPS*, 2021.
- [BLM20] Witold M. Bednorz, Rafał M. Łochowski, and Rafał Martynek. On tails of symmetric and totally asymmetric α -stable distributions. *arXiv:1802.00612 [math]*, November 2020.
- [BOFG20] Davis Blalock, Jose Javier Gonzalez Ortiz, Jonathan Frankle, and John Gutttag. What is the State of Neural Network Pruning? *arXiv:2003.03033 [cs, stat]*, March 2020.
- [CB18] Lénaïc Chizat and Francis Bach. On the global convergence of gradient descent for over-parameterized models using optimal transport. In S. Bengio, H. Wallach, H. Larochelle, K. Grauman, N. Cesa-Bianchi, and R. Garnett, editors, *Advances in Neural Information Processing Systems*, volume 31. Curran Associates, Inc., 2018.
- [CDE⁺21] Alexander Camuto, George Deligiannidis, Murat A Erdogdu, Mert Gürbüzbalaban, Umut Şimşekli, and Lingjiong Zhu. Fractal structure and generalization properties of stochastic optimization algorithms. In *NeurIPS*, 2021.
- [CWZ⁺21] Alexander Camuto, Xiaoyu Wang, Lingjiong Zhu, Chris Holmes, Mert Gürbüzbalaban, and Umut Şimşekli. Asymmetric heavy tails and implicit bias in gaussian noise injections. In *ICML*, 2021.
- [DBDFŞ20] Valentin De Bortoli, Alain Durmus, Xavier Fontaine, and Umut Şimşekli. Quantitative propagation of chaos for sgd in wide neural networks. In H. Larochelle, M. Ranzato, R. Hadsell, M. F. Balcan, and H. Lin, editors, *Advances in Neural Information Processing Systems*, volume 33, pages 278–288. Curran Associates, Inc., 2020.
- [DR17] Gintare Karolina Dziugaite and Daniel M. Roy. Computing Nonvacuous Generalization Bounds for Deep (Stochastic) Neural Networks with Many More Parameters than Training Data. *arXiv:1703.11008 [cs]*, October 2017.
- [EKT20] Bryn Elesedy, Varun Kanade, and Yee Whye Teh. Lottery Tickets in Linear Models: An Analysis of Iterative Magnitude Pruning. *arXiv:2007.08243 [cs, stat]*, August 2020.
- [FC19] Jonathan Frankle and Michael Carbin. The lottery ticket hypothesis: Finding sparse, trainable neural networks. In *International Conference on Learning Representations*, 2019.
- [FDRC20] Jonathan Frankle, Gintare Karolina Dziugaite, Daniel Roy, and Michael Carbin. Linear mode connectivity and the lottery ticket hypothesis. In Hal Daumé III and Aarti Singh, editors, *Proceedings of the 37th International Conference on Machine Learning*, volume 119 of *Proceedings of Machine Learning Research*, pages 3259–3269. PMLR, 13–18 Jul 2020.

- [Gal68] Robert G. Gallager. *Information Theory and Reliable Communication*. John Wiley & Sons, Inc., USA, 1968.
- [GCD12] Rémi Gribonval, Volkan Cevher, and Mike E Davies. Compressible distributions for high-dimensional statistics. *IEEE Transactions on Information Theory*, 58(8):5016–5034, 2012.
- [GŞZ21] Mert Gurbuzbalaban, Umut Şimşekli, and Lingjiong Zhu. The Heavy-Tail Phenomenon in SGD. In *ICML*, 2021.
- [HJRY20] Hattie Zhou, Janice Lan, Rosanne Liu, and Jason Yosinski. Deconstructing Lottery Tickets: Zeros, Signs, and the Supermask. *arXiv:1905.01067 [cs, stat]*, March 2020.
- [HJTW21] Daniel Hsu, Ziwei Ji, Matus Telgarsky, and Lan Wang. Generalization bounds via distillation. In *International Conference on Learning Representations*, 2021.
- [HM20] Liam Hodgkinson and Michael W. Mahoney. Multiplicative noise and heavy tails in stochastic optimization. *arXiv:2006.06293 [cs, math, stat]*, June 2020.
- [HPTD15] Song Han, Jeff Pool, John Tran, and William Dally. Learning both weights and connections for efficient neural network. In C. Cortes, N. Lawrence, D. Lee, M. Sugiyama, and R. Garnett, editors, *Advances in Neural Information Processing Systems*, volume 28. Curran Associates, Inc., 2015.
- [HZRS15] Kaiming He, Xiangyu Zhang, Shaoqing Ren, and Jian Sun. Deep residual learning for image recognition. *arXiv:1512.03385 [cs.CV]*, 2015.
- [HZS17] Yihui He, Xiangyu Zhang, and Jian Sun. Channel pruning for accelerating very deep neural networks. *arXiv:1707.06168 [cs]*, August 2017. *arXiv: 1707.06168*.
- [JMW08] Benjamin Jourdain, Sylvie Méléard, and Wojbor A Woyczynski. Nonlinear SDEs driven by Lévy processes and related PDEs. *Alea*, 4:29, 2008.
- [KL18] Ilja Kuzborskij and Christoph H. Lampert. Data-Dependent Stability of Stochastic Gradient Descent. *arXiv:1703.01678 [cs]*, February 2018.
- [KLG⁺21] Lorenz Kuhn, Clare Lyle, Aidan N. Gomez, Jonas Rothfuss, and Yarin Gal. Robustness to Pruning Predicts Generalization in Deep Neural Networks. *arXiv:2103.06002 [cs, stat]*, March 2021.
- [Kri09] Alex Krizhevsky. Learning multiple layers of features from tiny images. Technical report, 2009.
- [LCB10] Yann LeCun, Corinna Cortes, and CJ Burges. Mnist handwritten digit database. *ATT Labs [Online]*. Available: <http://yann.lecun.com/exdb/mnist>, 2, 2010.
- [LKD⁺17] Hao Li, Asim Kadav, Igor Durdanovic, Hanan Samet, and Hans Peter Graf. Pruning filters for efficient ConvNets. *arXiv:1608.08710 [cs]*, March 2017. *arXiv: 1608.08710*.
- [LMW20] Mingjie Liang, Mateusz B. Majka, and Jian Wang. Exponential ergodicity for SDEs and McKean-Vlasov processes with L^1 noise. *arXiv:1901.11125 [math]*, November 2020.
- [Lon17] Ben London. A pac-bayesian analysis of randomized learning with application to stochastic gradient descent. In I. Guyon, U. V. Luxburg, S. Bengio, H. Wallach, R. Fergus, S. Vishwanathan, and R. Garnett, editors, *Advances in Neural Information Processing Systems*, volume 30. Curran Associates, Inc., 2017.
- [LWZ81] Raoul LePage, Michael Woodroffe, and Joel Zinn. Convergence to a stable distribution via order statistics. *The Annals of Probability*, 9(4):624 – 632, 1981.
- [MM19] Charles H. Martin and Michael W. Mahoney. Traditional and Heavy-Tailed Self Regularization in Neural Network Models. *arXiv:1901.08276 [cs, stat]*, January 2019.

- [MMN18] Song Mei, Andrea Montanari, and Phan-Minh Nguyen. A mean field view of the landscape of two-layer neural networks. *Proceedings of the National Academy of Sciences*, 115(33):E7665–E7671, 2018.
- [MMO15] Mohammad Mohammadi, Adel Mohammadpour, and Hiroaki Ogata. On estimating the tail index and the spectral measure of multivariate α -stable distributions. *Metrika*, 78(5):549–561, 2015.
- [NBS18] Behnam Neyshabur, Srinadh Bhojanapalli, and Nathan Srebro. A PAC-Bayesian Approach to Spectrally-Normalized Margin Bounds for Neural Networks. *arXiv:1707.09564 [cs]*, February 2018.
- [Neu21] Gergely Neu. Information-Theoretic Generalization Bounds for Stochastic Gradient Descent. *arXiv:2102.00931 [cs, stat]*, February 2021.
- [Nol20] John P. Nolan. *Univariate Stable Distributions: Models for Heavy Tailed Data*. Springer, Switzerland, 2020.
- [NP21] Phan-Minh Nguyen and Huy Tuan Pham. A Rigorous Framework for the Mean Field Limit of Multilayer Neural Networks. *arXiv:2001.11443 [cond-mat, stat]*, May 2021.
- [NTS15] Behnam Neyshabur, Ryota Tomioka, and Nathan Srebro. Norm-based capacity control in neural networks. In *Conference on Learning Theory*, pages 1376–1401, 2015.
- [O’N20] James O’Neill. An overview of neural network compression. *arXiv:2006.03669 [cs, stat]*, August 2020.
- [PFF20] Stefano Peluchetti, Stefano Favaro, and Sandra Fortini. Stable behaviour of infinitely wide deep neural networks. In *Proceedings of the Twenty Third International Conference on Artificial Intelligence and Statistics*, volume 108, pages 1137–1146, 2020.
- [PGM⁺19] Adam Paszke, Sam Gross, Francisco Massa, Adam Lerer, James Bradbury, Gregory Chanan, Trevor Killeen, Zeming Lin, Natalia Gimelshein, Luca Antiga, Alban Desmaison, Andreas Kopf, Edward Yang, Zachary DeVito, Martin Raison, Alykhan Tejani, Sasank Chilamkurthy, Benoit Steiner, Lu Fang, Junjie Bai, and Soumith Chintala. Pytorch: An imperative style, high-performance deep learning library. In H. Wallach, H. Larochelle, A. Beygelzimer, F. d’Alché-Buc, E. Fox, and R. Garnett, editors, *Advances in Neural Information Processing Systems 32*, pages 8024–8035. Curran Associates, Inc., 2019.
- [RFC20] Alex Renda, Jonathan Frankle, and Michael Carbin. Comparing rewinding and fine-tuning in neural network pruning. *arXiv:2003.02389 [cs, stat]*, March 2020.
- [Rob55] Herbert Robbins. A remark on stirling’s formula. *The American Mathematical Monthly*, 62(1):26–29, 1955.
- [SAM⁺20] Taiji Suzuki, Hiroshi Abe, Tomoya Murata, Shingo Horiuchi, Kotaro Ito, Tokuma Wachi, So Hirai, Masatoshi Yukishima, and Tomoaki Nishimura. Spectral pruning: Compressing deep neural networks via spectral analysis and its generalization error. In *International Joint Conference on Artificial Intelligence*, pages 2839–2846, 2020.
- [SAN20] Taiji Suzuki, Hiroshi Abe, and Tomoaki Nishimura. Compression based bound for non-compressed network: unified generalization error analysis of large compressible deep neural network. In *International Conference on Learning Representations*, 2020.
- [SD15] Jorge F Silva and Milan S Derpich. On the characterization of ℓ_p -compressible ergodic sequences. *IEEE Transactions on Signal Processing*, 63(11):2915–2928, 2015.
- [ŠGN⁺19] Umut Şimşekli, Mert Gürbüzbalaban, Thanh Huy Nguyen, Gaël Richard, and Levent Sagun. On the Heavy-Tailed Theory of Stochastic Gradient Descent for Deep Neural Networks. *arXiv:1912.00018 [cs, math, stat]*, November 2019.
- [SS20] Justin Sirignano and Konstantinos Spiliopoulos. Mean field analysis of neural networks: A central limit theorem. *Stochastic Processes and their Applications*, 130(3):1820–1852, 2020.

- [§SDE20] Umut Şimşekli, Ozan Sener, George Deligiannidis, and Murat A Erdogdu. Hausdorff dimension, heavy tails, and generalization in neural networks. In H. Larochelle, M. Ranzato, R. Hadsell, M. F. Balcan, and H. Lin, editors, *Advances in Neural Information Processing Systems*, volume 33, pages 5138–5151. Curran Associates, Inc., 2020.
- [SSG19] Umut Simsekli, Levent Sagun, and Mert Gurbuzbalaban. A tail-index analysis of stochastic gradient noise in deep neural networks. In *International Conference on Machine Learning*, pages 5827–5837. PMLR, 2019.
- [SU20] Aastha M. Sathe and N. S. Upadhye. Estimation of the parameters of multivariate stable distributions. *Communications in Statistics - Simulation and Computation*, 0(0):1–18, July 2020. Publisher: Taylor & Francis _eprint: <https://doi.org/10.1080/03610918.2020.1784432>.
- [SZ15] Karen Simonyan and Andrew Zisserman. Very Deep Convolutional Networks for Large-Scale Image Recognition. *arXiv:1409.1556 [cs]*, April 2015.
- [Szn91] Alain-Sol Sznitman. Topics in propagation of chaos. In *Ecole d’été de probabilités de Saint-Flour XIX—1989*, pages 165–251. Springer, 1991.
- [§ZTG20] Umut Şimşekli, Lingjiong Zhu, Yee Whye Teh, and Mert Gürbüzbalaban. Fractional underdamped langevin dynamics: Retargeting sgd with momentum under heavy-tailed gradient noise. In *ICML*, 2020.
- [TNT18] G. Tzagkarakis, J. P. Nolan, and P. Tsakalides. Compressive Sensing of Temporally Correlated Sources Using Isotropic Multivariate Stable Laws. In *2018 26th European Signal Processing Conference (EUSIPCO)*, pages 1710–1714, September 2018. ISSN: 2076-1465.
- [TTR⁺20] Asma Teimouri, Mahbanoo Tata, Mohsen Rezapour, Rafal Kulik, and Narayanaswamy Balakrishnan. Asymptotic behavior of eigenvalues of variance-covariance matrix of a high-dimensional heavy-tailed lévy process. *Methodology and Computing in Applied Probability*, pages 1–23, 2020.
- [WGZ⁺21] Hongjian Wang, Mert Gürbüzbalaban, Lingjiong Zhu, Umut Şimşekli, and Murat A Erdogdu. Convergence rates of stochastic gradient descent under infinite noise variance. In *NeurIPS*, 2021.
- [Wu20] Yihong Wu. Lecture notes on information-theoretic methods for high-dimensional statistics, 2020.
- [WZG20] Chaoqi Wang, Guodong Zhang, and Roger Grosse. Picking winning tickets before training by preserving gradient flow. *arXiv:2002.07376 [cs, stat]*, August 2020.
- [YLWT17] Xiyu Yu, Tongliang Liu, Xinchao Wang, and Dacheng Tao. On compressing deep models by low rank and sparse decomposition. In *2017 IEEE Conference on Computer Vision and Pattern Recognition (CVPR)*, pages 67–76, Honolulu, HI, July 2017. IEEE.
- [ZFM⁺20] Pan Zhou, Jiashi Feng, Chao Ma, Caiming Xiong, Steven Chu Hong Hoi, and Weinan E. Towards theoretically understanding why SGD generalizes better than adam in deep learning. In H. Larochelle, M. Ranzato, R. Hadsell, M. F. Balcan, and H. Lin, editors, *Advances in Neural Information Processing Systems*, volume 33, pages 21285–21296. Curran Associates, Inc., 2020.
- [ZKV⁺20] Jingzhao Zhang, Sai Praneeth Karimireddy, Andreas Veit, Seungyeon Kim, Sashank Reddi, Sanjiv Kumar, and Suvrit Sra. Why are adaptive methods good for attention models? In H. Larochelle, M. Ranzato, R. Hadsell, M. F. Balcan, and H. Lin, editors, *Advances in Neural Information Processing Systems*, volume 33, pages 21285–21296. Curran Associates, Inc., 2020.
- [ZZL19] Yi Zhou, Huishuai Zhang, and Yingbin Liang. Understanding generalization error of sgd in nonconvex optimization. In *International Conference on Acoustics, Speech, and Signal Processing (ICASSP)*, May 2019.

Checklist

1. For all authors...
 - (a) Do the main claims made in the abstract and introduction accurately reflect the paper's contributions and scope? [\[Yes\]](#)
 - (b) Did you describe the limitations of your work? [\[Yes\]](#) For theoretical and practical limits of the work presented here see Section 6.
 - (c) Did you discuss any potential negative societal impacts of your work? [\[N/A\]](#) Our work is on the effective pruning of deep neural networks and how this relate to generalization. We expect the downstream effects of both the practical and theoretical aspects of our research to be positive in terms of future energy and storage use, as well as in the creation of robust algorithms. However, we understand that this is a high-dimensional issue and are happy to reconsider our opinion if the reviewers have any concerns.
 - (d) Have you read the ethics review guidelines and ensured that your paper conforms to them? [\[Yes\]](#)
2. If you are including theoretical results...
 - (a) Did you state the full set of assumptions of all theoretical results? [\[Yes\]](#) Please see Sections 3 and 4.
 - (b) Did you include complete proofs of all theoretical results? [\[Yes\]](#) Please see the supplementary material regarding our results in Sections 3 and 4.
3. If you ran experiments...
 - (a) Did you include the code, data, and instructions needed to reproduce the main experimental results (either in the supplemental material or as a URL)? [\[Yes\]](#) We provided these in the supplementary material.
 - (b) Did you specify all the training details (e.g., data splits, hyperparameters, how they were chosen)? [\[Yes\]](#) We provided as much detail as possible in Section 5 within space limits, we provided the rest in the supplementary material.
 - (c) Did you report error bars (e.g., with respect to the random seed after running experiments multiple times)? [\[No\]](#) As can be seen in Section 5 our results involve running the same experiment many times with a range of hyperparameters that are fairly close to each other. Our hypotheses are supported by the overall consistency and direction of these results. We believe that replicating these experiments numerous times would both be both too costly and would provide only marginal benefit.
 - (d) Did you include the total amount of compute and the type of resources used (e.g., type of GPUs, internal cluster, or cloud provider)? [\[Yes\]](#) We provided these in the supplementary material.
4. If you are using existing assets (e.g., code, data, models) or curating/releasing new assets...
 - (a) If your work uses existing assets, did you cite the creators? [\[Yes\]](#)
 - (b) Did you mention the license of the assets? [\[Yes\]](#)
 - (c) Did you include any new assets either in the supplemental material or as a URL? [\[Yes\]](#) The code base of this paper was made accessible through supplementary material.
 - (d) Did you discuss whether and how consent was obtained from people whose data you're using/curating? [\[N/A\]](#) We use publicly available and non-personal data only, namely MNIST and CIFAR10 datasets.
 - (e) Did you discuss whether the data you are using/curating contains personally identifiable information or offensive content? [\[N/A\]](#) We use publicly available and non-personal data only, namely MNIST and CIFAR10 datasets.
5. If you used crowdsourcing or conducted research with human subjects...
 - (a) Did you include the full text of instructions given to participants and screenshots, if applicable? [\[N/A\]](#) This item is not applicable for our research.
 - (b) Did you describe any potential participant risks, with links to Institutional Review Board (IRB) approvals, if applicable? [\[N/A\]](#) This item is not applicable for our research.
 - (c) Did you include the estimated hourly wage paid to participants and the total amount spent on participant compensation? [\[N/A\]](#) This item is not applicable for our research.

Heavy Tails in SGD and Compressibility of Overparametrized Neural Networks

SUPPLEMENTARY DOCUMENT

This document provides the supplementary material associated with the NeurIPS 2021 paper entitled “*Heavy Tails in SGD and Compressibility of Overparametrized Neural Networks*”. We organize the document as follows:

- Section **S1** describes the experimental setup used in our simulations, together with some additional experiment results and discussion.
- In Section **S2**, a generalization bound for an uncompressed network, given that this network is compressible, is presented.
- Section **S3** provides an upper-bound on the change in the network output when there is a small change in the network weights.
- In Section **S4**, the relation between compressibility and the tail index is discussed.
- Proofs of the main results of the paper are presented in Section **S5**.
- Finally, the technical lemmas are proved in Section **S6**.

S1 Details of the Experiments and Additional Results

Here we provide a more detailed explanation for our experimental setting, as well as the results and discussion we omitted from the main paper due to space restrictions.

S1.1 Datasets

The experiments were conducted in a supervised learning setting where the task is classification of images. Each model is trained on CIFAR10 [Kri09] and MNIST [LCB10] datasets. The MNIST is an image classification dataset where the data is comprised of 28×28 black and white handwritten digits, belonging to one class from 0 to 9. We use the traditional split defined in the dataset where there are 60000 training and 10000 test samples. CIFAR10 is also image classification dataset comprising 32×32 color images of objects or animals, making up 10 classes. There are 50000 training and 10000 test images, this is the split that we use in the experiments.

S1.2 Models

As described in the main text, in our experiments we use three models: a fully connected network with 4 hidden layers (FCN4), a fully connected network with 6 hidden layers (FCN6), and a convolutional neural network (CNN). Hidden layer widths are 2048 for the two FCN models. All networks include ReLU activation functions and none of them include batch normalization, dropout, residual layers, or any explicit regularization term in the loss function. The convolutional architecture for the CNN model for the CIFAR10 dataset progresses as below:

$$64, M, 128, M, 256, 256, M, 512, 512, M, 512, 512, M,$$

where integers stand for 2-dimensional convolutional layers (and the corresponding number of filters) with a kernel size of 3×3 , and M stands for 2×2 max-pooling with a stride of 2. Our CNN architecture follows that of VGG11 model [SZ15] except after the layers presented above we have only a single linear layer with a softmax output. For the MNIST experiment the first max-pooling layer was omitted as the dimensions of the MNIST images disallow the previous structure to be used. Table 1 includes the number of parameters for each model-dataset combination.

S1.3 Training and hyperparameters

All models were trained with SGD until 100% training accuracy and a training negative log-likelihood less than 5×10^{-5} is acquired, with constant learning rates and no momentum. The training

	FCN4	FCN6	CNN
CIFAR10	18,894,848	27,283,456	9,222,848
MNIST	14,209,024	22,597,632	9,221,696

Table 1: Parameter counts for all model-dataset combinations.

hyperparameters include two batch-sizes ($b = 50, 100$) and a variety of learning rates (η) to generate a large range of η/b values. See the table below for the range of η/b values created for each experiment setting. The ranges vary somewhat since different η/b values might lead to heavy-tailed behavior (or divergence) under different settings. Table 2 presents these ranges for all experiments. See the source code for all experiment settings that were presented in the main results.

	FCN4	FCN6	CNN
CIFAR10	5×10^{-5} to 2.7×10^{-3}	2.5×10^{-5} to 4×10^{-3}	1×10^{-5} to 1.5×10^{-3}
MNIST	5×10^{-5} to 1.14×10^{-2}	5×10^{-5} to 8.8×10^{-3}	1×10^{-5} to 6.35×10^{-3}

Table 2: η/b ranges for all experiments.

S1.4 Tail index estimation

We use the following multivariate tail index estimator proposed by [MMO15].

Theorem S5 ([MMO15, Corollary 2.4]). *Let $\{X_i\}_{i=1}^K$ be a collection of i.i.d. random vectors where each X_i is multivariate strictly stable with tail index α , and $K = K_1 \times K_2$. Define $Y_i \triangleq \sum_{j=1}^{K_1} X_{j+(i-1)K_1}$ for $i \in \llbracket 1, K_2 \rrbracket$. Then, the estimator*

$$\widehat{\frac{1}{\alpha}} \triangleq \frac{1}{\log K_1} \left(\frac{1}{K_2} \sum_{i=1}^{K_2} \log \|Y_i\| - \frac{1}{K} \sum_{i=1}^K \log \|X_i\| \right). \quad (\text{S1})$$

converges to $1/\alpha$ almost surely, as $K_2 \rightarrow \infty$.

This estimator has been used in previous research such as [SGN⁺19] and [TNT18]. We center the observations using the median values before the estimation. Using the alternative univariate tail index estimator [MMO15, Corollary 2.2] in the same paper has no qualitative effects on our results, an additional benefit of our choice is additional analyses it makes possible as presented in Section S1.6.2. Comparisons with alternative tail index estimators with symmetric α -stable assumption revealed no dramatic differences between various estimators [SU20].

S1.5 Pruning details

We first provide a review of the pruning methods we use. All three notions of pruning in our experiments correspond to the magnitude-wise ordering of certain parameters and the ‘pruning’ of a certain ratio of parameters that correspond to smallest magnitudes³. When the parameters that are pruned are the weight parameters themselves, this corresponds to magnitude-based pruning or *magnitude pruning* as known in the literature, which can be conducted layer-wise or globally [BOFG20]. *Singular value pruning*, as described here, corresponds to pruning of the smallest singular values (and, by implication, the related singular vectors) in the SVD of specific layers. To apply the SVD to CNN layers, we reshape the parameter tensors into matrices of shape (# channels) \times (# filters $\times 3 \times 3$). Lastly *node pruning* corresponds to the pruning of the whole columns in the weight matrices. Again, CNN counterpart of node pruning is open to interpretation; we choose to prune specific kernels according to the their norms.

Before any pruning is done, the parameters to be pruned are centered with the estimated median of the observations, in order to conform with our tail index estimation methodology. We chose median due

³Note that a more relaxed definition of pruning would be ‘systematic removal of model parameters’ to allow for different scoring methods in pruning [BOFG20]. However, we proceed with our specific definition since this allows us to communicate our theoretical and experimental results more concisely.

to its robustness against extreme observations especially with a small sample - however our results were qualitatively unchanged when the mean was used in the centering. After the pruning (in all three methods), the median was added to the pruned parameter vectors before testing the performance of the resulting model. Note that the median (or mean) was usually very small in norm and omitting centering made no qualitative effect on the results.

Lastly, while ‘remaining parameter ratio’ (κ) or ‘pruning ratio’ ($1 - \kappa$) are easy to interpret in the case of magnitude pruning or node pruning, in SVD κ would equal (number of singular value and vector parameters left) / (number of weight parameters in the layer), and pruning ratio would be determined accordingly.

S1.6 Additional results and discussion

Here we present additional results and discussion that were referenced in the main text but were not presented due to space restrictions.

S1.6.1 Causal interpretation of the relationships in question

An appropriate question regarding our theoretical and experimental findings would be: Is a causal interpretation of the hypothesized relations warranted? Although the relationship among training hyperparameters, parameter tail index, compressibility, and generalization is inevitably multifaceted, we believe that there are grounds to interpret the relations causally in this context.

To be more specific, [GŞZ21, Theorem 4, Proposition 5] shows that the tail index is fully determined by η , b , and the Hessian of the problem in the context of quadratic optimization: the tail index changes monotonically with respect to both η and b . In this paper we establish the relationship empirically in the context of neural networks, replicating the results presented in [GŞZ21]. We also show that the existence of heavy-tailed network parameters leads to compressibility (Theorems 1, 2, and 3), and thus to arbitrarily small perturbation in the network outputs when pruned (Lemma S1). We also demonstrate that the more compressible the network is, the smaller its generalization bound is (Theorem 4).

Using a different, geometric framework, [ŞSDE20, Appendix S1.2] (arxiv:2006.09313) experimentally demonstrated that a lower tail index leads to a better generalization, where they directly varied the tail index and monitored the generalization error, as the reviewer requested. Given these results and our experimental findings, we believe that a causal interpretation of the relationships in question is not without support.

Investigation of tail index and prunability with synthetic data. Experimental manipulation of tail index directly in the case of neural networks trained with real data is hard to formulate and conduct. However, to examine this issue further, we conducted a number of experiments with synthetic data.

In this setting, we created neural networks that were structural analogues of FCN6 networks presented in the original experiments, that is, feedforward neural networks of 6 hidden layers and a width of 2048 units for each hidden layer, with ReLU activation functions after each hidden layer. For the experiments, for each $\alpha_i \in \{1.50, 1.55, 1.60, \dots, 2.00\}$, we randomly sampled the parameters of these networks independently from a $\mathcal{S}_{\alpha}\mathcal{S}$ distribution with an α_i tail index parameter. After the sampling of the layer parameters, each layer was converted to a unit length vector, in order to avoid the possibly confounding effects of scale between different tail indices. This procedure excluded the much smaller final layer, which was sampled as in the initialization of the original experiments.

We also created random data for these experiments, in the shape of the MNIST training data, sampled independently from a standard normal distribution. For each network, the labels for these data were created by passing the synthetic data through the synthetic network and choosing the label with the maximum final value. Then, for each network created, we conducted layer-wise magnitude pruning for different values of κ , and evaluated the performance of the pruned versions of the networks with their original performances. This was repeated 10 times, and Figure ?? presents the mean of these accuracy values for each tail index (α) and pruning ratio ($1 - \kappa$) combination.

The results confirm our hypothesis: networks with lower tail indices are more prunable, that is, more robust to pruning in terms of performance. This replicates the conclusion of the original experiments, where a similar conclusion was reached with networks trained on real data. We leave the extension of

these experiments for different data generation schemes, layer structures, and pruning types to future work.

S1.6.2 Investigating the HML condition in synthetic experiments

Recall that in Figure 3 we examined, for a given relative compression error, whether lower tail index is associated with higher prunability. The results demonstrated that this was indeed the case. Here we compare our empirical results with some synthetic results to get additional insights regarding whether HML condition is actually observed in our networks.

For this experiment, we randomly sample tail indices $\alpha_i \sim \mathcal{U}(1.75, 2)$, where $i \in \{1, \dots, 250\}$. Then for each α_i , we sample three different ‘weight matrices’: $\mathbf{W}_{ind,i}, \mathbf{W}_{col,i}, \mathbf{W}_{lay,i} \in \mathbb{R}^{500 \times 500}$. The elements of $\mathbf{W}_{ind,i}$ are sampled independently from a $\mathcal{S}\alpha\mathcal{S}$ with tail index α_i ; this corresponds to the case where weight parameters are statistically independent as prescribed by the HML condition. On the other hand, columns of the $\mathbf{W}_{col,i}$ are independently sampled from a 500-dimensional multivariate *elliptically contoured* $\mathcal{S}\alpha\mathcal{S}$ with tail index α_i . A d -dimensional elliptically contoured multivariate $\mathcal{S}\alpha\mathcal{S}$ has the characteristic function

$$\mathbb{E}[\exp(i\langle \omega, X \rangle)] = \exp(-\|\omega\|^\alpha),$$

where $X, \omega \in \mathbb{R}^d$ and $\langle \cdot, \cdot \rangle$ stands for inner product. This means that while the columns of the matrix are independent, column elements can be correlated. Lastly, all elements of $\mathbf{W}_{lay,i}$ are sampled from a (500×500) -dimensional elliptically contoured multivariate $\mathcal{S}\alpha\mathcal{S}$, creating a case where all elements of the matrix can be correlated. We repeat the analysis presented in Figure 3 for all three sets of sampled synthetic layer weights, and present the results in Figure S1.

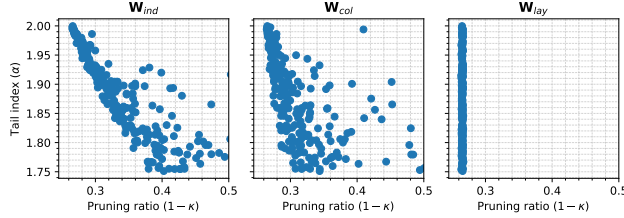


Figure S1: Tail index (α) vs. pruning ratio ($1 - \kappa$), with relative compression error = 0.1, for synthetically generated weight matrices.

The results demonstrate two interesting phenomena. First, a comparison of these results with Figure 3 shows that our empirical results show the most similarity with results obtained with $\mathbf{W}_{ind,i}$, showing support for the existence of the HML condition. Another observation is that as the layer parameters become correlated, the prunability advantage conferred by heavier tails disappears. This observation both supports the existence of HML condition in overparametrized neural networks and invites further discussion on the importance of propagation of chaos phenomenon in such architectures for compressibility and generalization [DBDFS20].

S1.6.3 Global magnitude pruning and node pruning results

In Figure S2 present the global magnitude pruning results for magnitude pruning. The results are qualitatively very similar to those of the layer-wise magnitude pruning. Figure S3 presents the results of node pruning on FCNs. As mentioned in the main text, the less impressive results might have to do with the layer widths not being sufficient for our theoretical conditions. A more favorable approach to structured pruning in FCNs would factor in the fact that removal of columns from a layer is also equivalent to the removal of corresponding rows from the previous layer. When computing the pruning ratio, factoring in these corresponding rows would produce more benevolent results. However, we have not done this in our experiments since this is not necessarily implied by our theory.

S1.7 Hardware and other resources

The experiments were conducted on an internal server of a research institute. Nvidia Titan X, 1080 Ti, and 1080 model GPU’s were used roughly equally in running the experiments. Our published

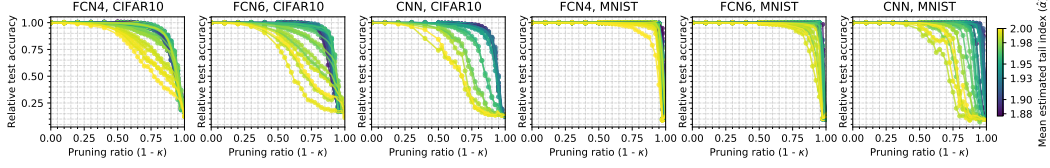


Figure S2: Relative test accuracy vs. pruning ratio for global magnitude pruning. Color: mean $\hat{\alpha}$.

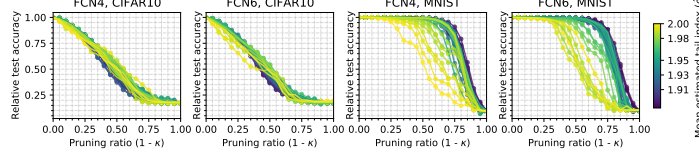


Figure S3: Relative test accuracy vs. pruning ratio for node pruning in FCNs. Color: mean $\hat{\alpha}$.

results involve 215 trained models, each of which included GPU-heavy workload, with an average completion time of approximately 2 hours. Around 30 models diverged (thus were not used in the results) and in most cases were trained for less than an hour. Total GPU-time could correspondingly be estimated to equal 460 hours. We also conducted tail index estimation and pruning experiments on these networks, however the computational load of these experiments are negligible compared to those of the training of the algorithms, with an estimated CPU time of 48 hours for all estimation and pruning tasks that were published.

As can be seen in the accompanying code, the experiments were conducted using Python programming language. The deep learning framework PyTorch [PGM⁺19] as well as some of its tutorials⁴ were used in implementing the experiments.

S2 Generalization bound for the uncompressed network

In this section, in the continuation of Section 4, we establish a generalization bound for an uncompressed network, if this network is compressible using the layer-wise magnitude pruning strategy.

Theorem S6. Assume **H1** holds. Then for $n: n/\log(n) \geq \max(9L, 81\varepsilon^{-2\kappa})$, $\{d_l\}_{l=1}^L: d_l \geq d_{l,0}$ and $d \geq 10$, and any $\delta, \tau > 0$, with probability at least $1 - 2e^{-d/2} - \delta - \epsilon$,

$$\mathcal{R}_0(\mathbf{w}) \leq \hat{\mathcal{R}}_\tau(\mathbf{w}) + \max\left(2, 24\rho_\varepsilon(\kappa, d)\mathcal{L}(\tau, \delta)R(\delta)/\sqrt{d}\right)\sqrt{d\log(n)/n}. \quad (\text{S2})$$

where $R(\delta)$ and $\mathcal{L}(\tau, \delta)$ are defined in (7), $\kappa := \frac{1}{d} \sum_{l=1}^L \lceil \kappa_l d_l \rceil$,

$$\begin{aligned} \rho_\varepsilon(\kappa, d) &:= \min\left(\varepsilon^{1-\kappa} \exp\left(h_b(\kappa) + h_b^{(1)}(\kappa, d)\right), 1\right) \leq \min(3\varepsilon^{1-\kappa}, 1), \\ h_b^{(1)}(\kappa, d) &:= \frac{\lceil d/2 \rceil}{d} \max(h_b(\lceil \kappa d/2 \rceil / \lceil d/2 \rceil), h_b(\lfloor \kappa d/2 \rfloor / \lfloor d/2 \rfloor)). \end{aligned}$$

Note that the function $h_b^{(1)}(\kappa, d) \leq \log(2)(1/2 + 1/d)$. Hence $\varepsilon^{1-\kappa} e^{h_b(\kappa) + h_b^{(1)}(\kappa, d)} \leq \varepsilon^{1-\kappa} e^{\log(2)(3/2 + 1/d)} \leq 3\varepsilon^{1-\kappa}$, for $d \geq 12$. Besides, $\rho_\varepsilon(1, d) = 1$ and $\rho_\varepsilon(0, d) = \varepsilon$. Moreover, when both d and κd are even numbers, then $h_b^{(1)}(\kappa, d) = \frac{1}{2}h_b(\kappa)$ and $\rho_\varepsilon(\kappa) := \rho_\varepsilon(\kappa, d)$ is increasing with respect to κ . To show the latter claim, consider the derivative of $g(\kappa) := \varepsilon^{1-\kappa} \exp(\frac{3}{2}h_b(\kappa))$ with respect to κ . This derivative is equal to zero at $\kappa^* = 1/(1 + \varepsilon^{2/3})$ and is positive for $\kappa < \kappa^*$. In addition, $g(\kappa^*) = (1 + \varepsilon^{2/3})^{3/2} > 1$. Hence, $\rho_\varepsilon(\kappa) = \min(g(\kappa), 1)$ is increasing with respect to κ . In Figure S4, $\rho_\varepsilon(\kappa) = \min(\varepsilon^{1-\kappa} \exp(\frac{3}{2}h_b(\kappa)), 1)$, together with its upper bound $\min(3\varepsilon^{1-\kappa}, 1)$ are plotted for different values of ε .

⁴[HTTPS://GITHUB.COM/PYTORCH/VISION/BLOB/MASTER/TORCHVISION/MODELS/VGG.PY](https://github.com/pytorch/vision/blob/master/torchvision/models/vgg.py)

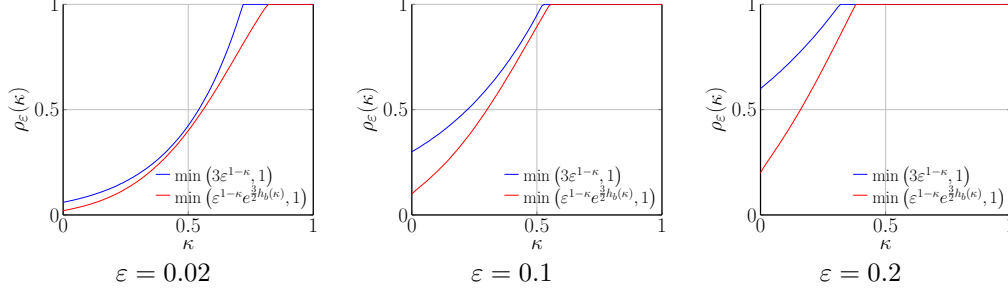


Figure S4: $\rho_\varepsilon(\kappa)$ for different values of ε .

It can be observed that if a network is more compressible, then not only the compressed network, but also the original network has a better generalization bound. This result is consistent with the findings of [HJTW21, KLG⁺21]. In [HJTW21], it is shown that if two networks are “close” enough, a good generalization bound on one of them, would imply a good bound on the other one as well. In [KLK⁺21], it is shown that “prunability” of a network captures well the generalization property of the network.

Finally, it should be noted that when the weights of the network follow a stable distribution, similar results to Corollary 1 can be established for the original network.

S3 Perturbation Bound

The goal of pruning is to find compressed weights $\hat{\mathbf{w}}$ with low dimensionality that are close enough to the original weights \mathbf{w} , which is measured in this work by the relative error $\|\hat{\mathbf{w}} - \mathbf{w}\|/\|\mathbf{w}\|$. The following perturbation result guarantees that such pruning strategies also result in small perturbations on the output of the network. The proof is based on the technique given in [NBS18].

Lemma S1. *Let $\mathbf{w}, \hat{\mathbf{w}} \in \mathbb{R}^d$ be two fully connected neural networks. Assume that there exists $\{\varepsilon_l\}_{l=1}^L$: $\varepsilon_l \geq 0$, such that $\|\hat{\mathbf{w}}_l - \mathbf{w}_l\| \leq \varepsilon_l \|\mathbf{w}_l\|$, for all $l \in \llbracket 1, L \rrbracket$. Then, the following inequality holds:*

$$\|f_{\hat{\mathbf{w}}}(\mathbf{x}) - f_{\mathbf{w}}(\mathbf{x})\| \leq B \left[\prod_{l=1}^L (1 + \varepsilon_l) - 1 \right] \left[\prod_{l=1}^L \|\mathbf{w}_l\| \right], \quad (\text{S3})$$

for all $\mathbf{x} \in \mathcal{X}_B$. In particular, if $\varepsilon_l = \varepsilon$ for all layers and $\|\mathbf{w}\| \leq R$, then

$$\|f_{\hat{\mathbf{w}}}(\mathbf{x}) - f_{\mathbf{w}}(\mathbf{x})\| \leq B \left[(1 + \varepsilon)^L - 1 \right] \left(R/\sqrt{L} \right)^L. \quad (\text{S4})$$

For derivation of the above bound on the network outputs, the worst case in the propagation of the errors of each layer is assumed, which results into an exponential dependence on the depth of the network, similarly to [NBS18].

S4 Compression rate and tail index

In this work, different pruning strategies have been investigated by exploiting the compressibility properties of heavy-tailed distributions. In this section, we show that moreover, in some certain sense, heavier-tailed distributions are more compressible. However, we must underline that this result is neither comprehensive, nor directly usable in our framework, as we will discuss after stating it.

Before stating the result, let us define the following quantity. For $\varepsilon > 0$ and $\mathbf{w} \in \mathbb{R}^d$, let

$$\kappa_p(\mathbf{w}, \varepsilon) := \min \left\{ \kappa : \left(\|\mathbf{w}^{(\kappa d)} - \mathbf{w}\|_p / \|\mathbf{w}\|_p \right) \leq \varepsilon \right\}. \quad (\text{S5})$$

Proposition S1. *Suppose that $\mathbf{w}_1 \in \mathbb{R}^d$ and $\mathbf{w}_2 \in \mathbb{R}^d$ are independent vectors of i.i.d. heavy-tailed random variables with tail indices α_1 and α_2 , respectively. If $\alpha_1 > \alpha_2$, then for any $\kappa, \varepsilon, \delta > 0$ and $p < \max(\alpha_1, \alpha_2)$, there exists $d_0(\delta)$, such that for $d \geq d_0(\delta)$,*

$$\mathbb{E} \left[\|\mathbf{w}_1^{(\kappa d)} - \mathbf{w}_1\|_p / \|\mathbf{w}_1\|_p \right] + \delta > \mathbb{E} \left[\|\mathbf{w}_2^{(\kappa d)} - \mathbf{w}_2\|_p / \|\mathbf{w}_2\|_p \right], \quad (\text{S6})$$

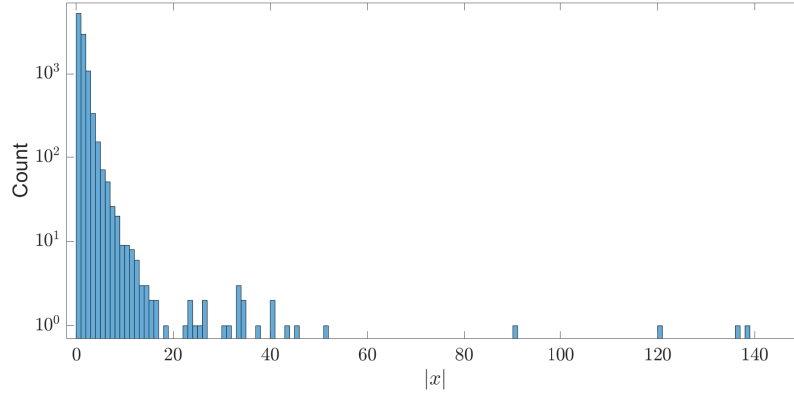


Figure S5: Histogram of $|x|$ for a sequence of i.i.d. random variables distributed according to $\mathcal{S}_\alpha \mathcal{S}(1)$, where $\alpha = 1.7$.

and

$$\mathbb{E}[\kappa_p(\mathbf{w}_1, \varepsilon)] + \delta > \mathbb{E}[\kappa_p(\mathbf{w}_2, \varepsilon)]. \quad (\text{S7})$$

The above proposition shows that for a fixed p -norm of the normalized compression error with $p < \alpha$, the heavier-tailed distributions are more compressible. The caveat here is that for $p \geq \max(\alpha_1, \alpha_2)$, all terms in (S6) and (S7) go to zero due to Lemma S2 and hence (S6) and (S7) trivially hold. Therefore, unfortunately we cannot use Proposition S1 in our framework since we are mainly interested in the case where $p \geq \max(\alpha_1, \alpha_2)$. Investigating the level of compressibility as a function of the tail index is a natural next step for our study.

S5 Proofs of the Main Results

In this section we provide proofs of our main results. We shall begin with stating the following result from [GCD12], which will be repeatedly used in our proofs.

S5.1 Existing Theoretical Results

Many of our results are based on the compressibility of i.i.d. instances of heavy-tailed random variables. Here, we state a known result regarding this fact.

Lemma S2 ([GCD12, Proposition 1, Part 2]). *Let $x \in \mathbb{R}$ be a random variable and assume that $\mathbb{E}|x|^\alpha = \infty$ for some $\alpha \in \mathbb{R}_+$. Then for all $p \geq \alpha$, $0 < \kappa \leq 1$ and any sequence κ_d such that $\lim_{d \rightarrow \infty} \frac{\kappa_d}{d} = \kappa$, the following identity holds almost surely:*

$$\lim_{d \rightarrow \infty} \left(\|\mathbf{x}^{(\kappa_d)} - \mathbf{x}\|_p / \|\mathbf{x}\|_p \right) = 0, \quad (\text{S8})$$

where $\mathbf{x} = (x_1, \dots, x_d)$ is a vector of i.i.d. random variables of length d .

A similar result was concurrently proven in [AUM11]. As stated before, this result informally states that for a large vector of i.i.d. heavy-tailed random variables, the norm of the vector is mainly determined by a small fraction of its entries. To show this visually, we have generated 10^4 i.i.d. random variables $\{x_i\}_i$ with $\mathcal{S}_\alpha \mathcal{S}(1)$ distribution where $\alpha = 1.7$. Then, we have plotted the histogram of $|x|$ in Figure S5. As can be seen in the figure, the norm of the whole vector is mainly determined by few number of samples.

S5.2 Proof of Theorem 1

Proof. (i) As $\{d_l\}_{l=1}^L$ grow, due to HML condition and assumptions of this part of the theorem, \mathbf{w} converges in distribution to a heavy-tailed random vector, denoted as $\mathbf{x} = (x_1, \dots, x_d) \in \mathbb{R}^d$,

with i.i.d. elements and tail index $\alpha \in (0, 2)$. Hence, for any $\epsilon > 0$, $\varepsilon > 0$, $\kappa \in (0, 1)$, and $p \geq \alpha$ there exists $\{d'_{l,0}\}_{l=1}^L : d'_{l,0} \in \mathbb{N}$ such that for $d_l \geq d'_{l,0}$, $l \in \llbracket 1, L \rrbracket$,

$$\mathbb{P}\left[\left(\|\mathbf{x}^{(\kappa d)} - \mathbf{x}\|_p / \|\mathbf{x}\|_p\right) \leq \varepsilon\right] - \mathbb{P}\left[\left(\|\mathbf{w}^{(\kappa d)} - \mathbf{w}\|_p / \|\mathbf{w}\|_p\right) \leq \varepsilon\right] \leq \epsilon. \quad (\text{S9})$$

Moreover due to Lemma S2, there exists $d''_0 \in \mathbb{N}$ such that for $d \geq d''_0$,

$$\mathbb{P}\left[\left(\|\mathbf{x}^{(\kappa d)} - \mathbf{x}\|_p / \|\mathbf{x}\|_p\right) \leq \varepsilon\right] = 1 \quad (\text{S10})$$

The results follows from (S9) and (S10) and by choosing $d_{l,0} \geq d'_{l,0}$, for $l \in \llbracket 1, L \rrbracket$, such that $\sum_{l=1}^L d_{l,0} \geq d''_0$.

- (ii) The proof is similar to the previous part. As $\{d_l\}_{l=1}^L$ grow, due to HML condition, for $l \in \llbracket 1, L \rrbracket$, \mathbf{w}_l converges in distribution to a heavy-tailed random vector, denoted as $\mathbf{x}_l = (x_{l,1}, \dots, x_{l,d_l}) \in \mathbb{R}^{d_l}$, with i.i.d. elements and tail index $\alpha_l \in (0, 2)$. Hence, for any $\epsilon > 0$, $\{\varepsilon_l\}_{l=1}^L : \varepsilon_l > 0$, $\{\kappa_l\}_{l=1}^L : \kappa_l \in (0, 1)$, and $p \geq \max_l \alpha_l$ there exists $\{d'_{l,0}\}_{l=1}^L : d'_{l,0} \in \mathbb{N}$ such that for $d_l \geq d'_{l,0}$, $l \in \llbracket 1, L \rrbracket$,

$$\mathbb{P}\left[\left(\|\mathbf{x}_l^{(\kappa_l d_l)} - \mathbf{x}_l\|_p / \|\mathbf{x}_l\|_p\right) \leq \varepsilon_l\right] - \mathbb{P}\left[\left(\|\mathbf{w}_l^{(\kappa_l d_l)} - \mathbf{w}_l\|_p / \|\mathbf{w}_l\|_p\right) \leq \varepsilon_l\right] \leq \epsilon. \quad (\text{S11})$$

Moreover due to Lemma S2, there exists $\{d''_{l,0}\}_{l=1}^L : d''_{l,0} \in \mathbb{N}$ such that for $d_l \geq d''_{l,0}$,

$$\mathbb{P}\left[\left(\|\mathbf{x}_l^{(\kappa_l d_l)} - \mathbf{x}_l\|_p / \|\mathbf{x}_l\|_p\right) \leq \varepsilon_l\right] = 1 \quad (\text{S12})$$

The results follows from (S12) and (S11) and by choosing $d_{l,0} \geq \max(d'_{l,0}, d''_{l,0})$.

□

S5.3 Proof of Theorem 2

Proof. Fix $l \in \llbracket 2, L-1 \rrbracket$ and recall that $\mathbf{W}_l \in \mathbb{R}^{h_l \times h_{l-1}}$ with $d_l = h_l \times h_{l-1}$. Define

$$\mathbf{X}_l := \frac{1}{h_l^{2/\alpha_l}} \mathbf{W}_l^\top \mathbf{W}_l \quad (\text{S13})$$

and denote the eigenvalues of \mathbf{X}_l by $\lambda_l = [\lambda_{l,1}, \dots, \lambda_{l,h_{l-1}}]$.

Let $\mathbf{U}_l \in \mathbb{R}^{h_l \times h_{l-1}}$ be a matrix whose entries are independent and identically distributed from a symmetric stable distribution with tail index α_l . Note that \mathbf{W}_l converges in distribution to \mathbf{U}_l , as network dimension goes to infinity, due to HML condition and the assumptions of the theorem. Similarly, define

$$\mathbf{X}'_l := \frac{1}{h_l^{2/\alpha_l}} \mathbf{U}_l^\top \mathbf{U}_l \quad (\text{S14})$$

and denote the eigenvalues of \mathbf{X}'_l by $\lambda'_l = [\lambda'_{l,1}, \dots, \lambda'_{l,h_{l-1}}]$.

As \mathbf{W}_l converges in distribution to \mathbf{U}_l , then $\lambda_{l,k}$ also weakly converges to $\lambda'_{l,k}$, due to Weyl's inequality ([Bha97, Page 63]). Hence, for any $\epsilon > 0$, $\{\varepsilon_l\}_{l=2}^{L-1} : \varepsilon_l > 0$, and $\{\kappa_l\}_{l=2}^{L-1} : \kappa_l \in (0, 1)$, there exists $\{\hat{h}_{l,0}\}_{l=1}^{L-1}$, such that for every $l \in \llbracket 2, L-1 \rrbracket$, and $h_i \geq \hat{h}_{i,0}$ for all $i \in \llbracket 1, l \rrbracket$, the following holds

$$\left| \mathbb{P}\left[\frac{\|\lambda_i^{(\kappa_i h_{i-1})} - \lambda_i\|_p}{\|\lambda_i\|_p} \leq \varepsilon_i^2\right] - \mathbb{P}\left[\frac{\|\lambda'_i^{(\kappa_i h_{i-1})} - \lambda'_i\|_p}{\|\lambda'_i\|_p} \leq \varepsilon_i^2\right] \right| \leq \frac{\epsilon}{2}. \quad (\text{S15})$$

Moreover, since each $[\mathbf{U}]_{i,j}$ is independent and identically distributed from a symmetric stable distribution with tail index α_l , by [TTR⁺20, Theorem 2.7], as $h_l \rightarrow \infty$, for each $k = 1, \dots, h_{l-1}$, the eigenvalue $\lambda'_{l,k}$ weakly converges to a random variable $\xi_{l,k}$, where the collection $\{\xi_{l,k}\}_{k=1}^{h_{l-1}}$ is independent and identically distributed from a positive stable distribution with tail index $\alpha_l/2$.

Denote by $\xi_l := [\xi_{l,1}, \dots, \xi_{l,h_{l-1}}] \in \mathbb{R}^{h_{l-1}}$ the random vector containing the limiting i.i.d. random variables.

We will now construct a sequence of $\{h_{l,0}\}_{l=1}^{L-1}$ such that the claims will follow for $h_l \geq h_{l,0}$. Let us start from the second layer, i.e., set $l = 2$. Then, by Lemma S2, for any $\varepsilon_2 > 0$, $\kappa_2 \in (0, 1)$, and $p \geq \alpha_2/2$, there exists $h'_{1,0} \in \mathbb{N}_+$, such that $h_1 \geq h'_{1,0}$ implies:

$$\mathbb{P} \left[\frac{\|\xi_2^{(\kappa_2 h_1)} - \xi_2\|_p}{\|\xi_2\|_p} \leq \varepsilon_2^2 \right] = 1. \quad (\text{S16})$$

Let $h_{1,0} = h'_{1,0} \vee \hat{h}_{1,0}$. Having fixed $h_1 \geq h_{1,0}$, we now iterate the following argument from $l = 2$ to $l = L - 1$ sequentially. Due to the weak convergence of the eigenvalues, we have:

$$\lim_{h_l \rightarrow \infty} \mathbb{P} \left[\frac{\|\lambda_l^{(\kappa_l h_{l-1})} - \lambda_l'\|_p}{\|\lambda_l'\|_p} \leq \varepsilon_l^2 \right] = \mathbb{P} \left[\frac{\|\xi_l^{(\kappa_l h_{l-1})} - \xi_l\|_p}{\|\xi_l\|_p} \leq \varepsilon_l^2 \right] \quad (\text{S17})$$

$$= 1. \quad (\text{S18})$$

Hence, combining with (S15), for any $\epsilon > 0$, there exists $h''_{l,0} \in \mathbb{N}_+$, such that $h_l \geq h''_{l,0} \vee \hat{h}_{l,0}$ implies

$$\mathbb{P} \left[\frac{\|\lambda_l^{(\kappa_l h_{l-1})} - \lambda_l\|_p}{\|\lambda_l\|_p} \leq \varepsilon_l^2 \right] \geq 1 - \epsilon. \quad (\text{S19})$$

If $l = L - 1$, set $h_{l,0} = h''_{l,0} \vee \hat{h}_l \vee h_{l-1}$. If $l \leq L - 2$, repeat the previous argument to find a $h'_{l,0}$, such that $h_l \geq h'_{l,0}$ implies

$$\mathbb{P} \left[\frac{\|\xi_{l+1}^{(\kappa_{l+1} h_l)} - \xi_{l+1}\|_p}{\|\xi_{l+1}\|_p} \leq \varepsilon_{l+1}^2 \right] = 1, \quad (\text{S20})$$

and set $h_{l,0} = h'_{l,0} \vee h''_{l,0} \vee \hat{h}_{l,0} \vee h_{l-1}$. This proves the first claim.

To prove the second claim, first notice that we can set $p = 1$ as $\max_l \alpha_l < 2$, hence $p = 1 \geq \alpha_l/2$ for all l . Now, fix $l \in \llbracket 2, L - 1 \rrbracket$, and for a given h_{l-1} and h_l , consider the singular value decomposition of \mathbf{W}_l as:

$$\mathbf{W}_l = \mathbf{U} \Sigma \mathbf{V}^\top, \quad (\text{S21})$$

and define $\mathbf{W}_l^{[\kappa_l h_{l-1}]} := \mathbf{U} \Sigma^{(\kappa_l h_{l-1})} \mathbf{V}^\top$, where $\Sigma^{(\kappa_l h_{l-1})}$ is the diagonal matrix whose diagonal entries contain the $\lceil \kappa_l h_{l-1} \rceil$ largest singular values (i.e., prune the diagonal part of Σ). By using (S19) and the fact that the Schatten 2-norm coincides with the Frobenius norm, we have:

$$\|\mathbf{W}_l\|^2 = h_l^{1/\alpha_l} \|\lambda_l\|_1, \quad \text{and} \quad \|\mathbf{W}_l^{[\kappa_l h_{l-1}]} - \mathbf{W}_l\|^2 = h_l^{1/\alpha_l} \|\lambda_l^{(\kappa_l h_{l-1})} - \lambda_l\|_1. \quad (\text{S22})$$

Hence, we conclude that for $h_l \geq h_{l,0}$, the following inequality holds for $l \in \llbracket 2, L - 1 \rrbracket$:

$$\mathbb{P} \left[\frac{\|\mathbf{W}_l^{[\kappa_l h_{l-1}]} - \mathbf{W}_l\|}{\|\mathbf{W}_l\|} \leq \varepsilon_l \right] \geq 1 - \epsilon. \quad (\text{S23})$$

This concludes the proof. \square

S5.4 Proof of Theorem 3

Proof. For $l \in \llbracket 2, L \rrbracket$, let $v_{l,i} = \|\mathbf{W}_l(i)\|_p$, where $\mathbf{W}_l(i) \in \mathbb{R}^{h_l}$ is the i -th column of $\mathbf{W}_l \in \mathbb{R}^{h_l \times h_{l-1}}$ for $i \in \llbracket 1, h_{l-1} \rrbracket$. Note that by definition, for any $\kappa_l \in (0, 1)$

$$\|\mathbf{v}_l\|_p = \|\mathbf{w}_l\|_p, \quad \text{and} \quad \|\mathbf{v}_l^{(\kappa_l h_{l-1})} - \mathbf{v}_l\|_p = \|\mathbf{w}_l^{\{\kappa_l h_{l-1}\}, p} - \mathbf{w}_l\|_p.$$

Hence, it suffices to show that for any $\epsilon > 0$ and $\varepsilon_l > 0$, there exists $h_{l-1,0}$ such that for $h_{l-1} \geq h_{l-1,0}$,

$$\mathbb{P} \left[\left(\|\mathbf{v}_l^{(\kappa_l h_{l-1})} - \mathbf{v}_l\|_p \right) / \|\mathbf{v}_l\|_p \leq \varepsilon_l \right] \geq 1 - \epsilon. \quad (\text{S24})$$

As network dimensions grow, due to HML condition, $w_{l,j}, j \in \llbracket 1, d_l \rrbracket$ converges in distribution to an i.i.d. heavy-tailed random variable with tail index α_l . Hence, as $\{h_{l-1}\}_{l=2}^L$ grows, $v_{l,i}$ also converges in distribution to a heavy-tailed random variable, denoted as $\mathbf{x}_l = (x_{l,1}, \dots, x_{l,h_{l-1}}) \in \mathbb{R}^{h_{l-1}}$, with i.i.d. elements and tail index $\alpha_l \in (0, 2)$. Thus, there exists $\{h'_{l-1,0}\}_{l=2}^L: h'_{l-1,0} \in \mathbb{N}$ such that for $h_{l-1} \geq h'_{l-1,0}, l \in \llbracket 2, L \rrbracket$,

$$\mathbb{P}\left[\left(\|\mathbf{x}_l^{(\kappa_l h_{l-1})} - \mathbf{x}_l\|_p / \|\mathbf{x}_l\|_p\right) \leq \varepsilon_l\right] - \mathbb{P}\left[\left(\|\mathbf{v}_l^{(\kappa_l h_{l-1})} - \mathbf{v}_l\|_p / \|\mathbf{v}_l\|_p\right) \leq \varepsilon_l\right] \leq \epsilon. \quad (\text{S25})$$

Moreover due to Lemma S2, there exists $\{h''_{l-1,0}\}_{l=2}^L: h''_{l-1,0} \in \mathbb{N}$ such that for $h_{l-1} \geq h''_{l-1,0}$,

$$\mathbb{P}\left[\left(\|\mathbf{x}_l^{(\kappa_l h_{l-1})} - \mathbf{x}_l\|_p / \|\mathbf{x}_l\|_p\right) \leq \varepsilon_l\right] = 1 \quad (\text{S26})$$

The results follows from (S12) and (S11) and by choosing $h_{l-1,0} \geq \max(h'_{l-1,0}, h''_{l-1,0})$. \square

S5.5 Proof of Theorem 4

Let

$$D(y, f_{\mathbf{w}}(\mathbf{x})) := f_{\mathbf{w}}(\mathbf{x})[y] - \max_{j \neq y} f_{\mathbf{w}}(\mathbf{x})[j].$$

Define the surrogate loss function $\ell_{\gamma, \tau}: \mathcal{Y} \times \mathcal{Y} \mapsto [0, 1]$, with margin loss $\gamma \geq 0$ and continuity margin $\tau > 0$, for the multiclass classifier $f_{\mathbf{w}}$ as:

$$\ell_{\gamma, \tau}(y, f_{\mathbf{w}}(\mathbf{x})) := \begin{cases} 1, & \text{if } D(y, f_{\mathbf{w}}(\mathbf{x})) \leq \gamma, \\ 1 - \frac{D(y, f_{\mathbf{w}}(\mathbf{x})) - \gamma}{\tau}, & \text{if } \gamma < D(y, f_{\mathbf{w}}(\mathbf{x})) \leq \gamma + \tau, \\ 0, & \text{if } \gamma + \tau < D(y, f_{\mathbf{w}}(\mathbf{x})). \end{cases} \quad (\text{S27})$$

Note that $\ell_{\gamma}(y, f_{\mathbf{w}}(\mathbf{x})) = \ell_{\gamma, 0}(y, f_{\mathbf{w}}(\mathbf{x}))$. Population and empirical risks of a hypothesis \mathbf{w} are denoted by $\mathcal{R}_{\gamma, \tau}(\mathbf{w})$ and $\hat{\mathcal{R}}_{\gamma, \tau}(\mathbf{w})$, respectively.

Proof. Recall that for all $l \in \llbracket 1, L \rrbracket$, $\hat{\mathbf{w}}_l := \mathbf{w}_l^{(\kappa_l d_l)}$. Denote by A the event that \mathbf{w} is compressible, i.e. when for all $l \in \llbracket 1, L \rrbracket$, $\|\hat{\mathbf{w}}_l - \mathbf{w}_l\| \leq \varepsilon \|\mathbf{w}_l\|$. Denote its complement by A^C and note that $\mathbb{P}(A^C) \leq \epsilon$, where the probability is with respect to $P_{S, \mathbf{w}}$.

Fix $\delta, \tau > 0$. We show that with probability of at least $1 - 2e^{-\kappa d/2} - \delta - \epsilon$:

$$\mathcal{R}_{0, \tau}(\hat{\mathbf{w}}) \leq \hat{\mathcal{R}}_{0, \tau}(\hat{\mathbf{w}}) + \left(12\mathcal{L}(\tau, \delta)R(\delta) + \sqrt{d}\right) \sqrt{\frac{(\kappa + \epsilon_{\kappa})d \log(n)}{n}}, \quad (\text{S28})$$

and moreover $\|\mathbf{w}\| \leq R(\delta)$ and $\|\hat{\mathbf{w}}_l - \mathbf{w}_l\| \leq \varepsilon \|\mathbf{w}_l\|$ for all $l \in \llbracket 1, L \rrbracket$, simultaneously. Then, under the latter two conditions,

$$\begin{aligned} \mathcal{R}_{0, \tau}(\hat{\mathbf{w}}) &\leq \mathcal{R}_{0, \tau}(\hat{\mathbf{w}}), \\ \hat{\mathcal{R}}_{0, \tau}(\hat{\mathbf{w}}) &\leq \hat{\mathcal{R}}_{\gamma(\delta, \tau)}(\mathbf{w}), \end{aligned}$$

using Lemma S1, Definition S27, and Lemma S3 that bounds the Lipschitz coefficient of the network. This completes the proof.

Lemma S3. Suppose that for $l \in \llbracket 1, L \rrbracket$ and a given $v_l > 0$, we have $\|\mathbf{w}_l - \mathbf{w}'_l\| \leq v_l$.

i. Then, for any (\mathbf{x}, y) , the following relations hold:

$$\begin{aligned} \|f_{\mathbf{w}}(\mathbf{x}) - f_{\mathbf{w}'}(\mathbf{x})\| &\leq B \prod_{l=1}^L (\|\mathbf{w}_l\| + v_l) - B \prod_{l=1}^L \|\mathbf{w}_l\|, \\ |\ell_{0, \tau}(y, f_{\mathbf{w}}(\mathbf{x})) - \ell_{0, \tau}(y, f_{\mathbf{w}'}(\mathbf{x}))| &\leq \frac{\sqrt{2}}{\tau} \|f_{\mathbf{w}}(\mathbf{x}) - f_{\mathbf{w}'}(\mathbf{x})\|. \end{aligned}$$

ii. In particular, if $v_l = v \leq R/\sqrt{L}$ for $l \in \llbracket 1, L \rrbracket$ and if $\|\mathbf{w}\| \leq R$, then

$$\begin{aligned} \|f_{\mathbf{w}}(\mathbf{x}) - f_{\mathbf{w}'}(\mathbf{x})\| &\leq BL \left(\frac{2R}{\sqrt{L}} \right)^{L-1} v, \\ |\ell_{0,\tau}(y, f_{\mathbf{w}}(\mathbf{x})) - \ell_{0,\tau}(y, f_{\mathbf{w}'}(\mathbf{x}))| &\leq \frac{BL\sqrt{2}}{\tau} \left(\frac{2R}{\sqrt{L}} \right)^{L-1} v =: \mathcal{L}(\tau, \delta)v. \end{aligned}$$

Hence, it remains to show (S28) together with the conditions $\|\mathbf{w}\| \leq R(\delta)$ and $\|\hat{\mathbf{w}}_l - \mathbf{w}_l\| \leq \varepsilon \|\mathbf{w}_l\|$, for $l \in \llbracket 1, L \rrbracket$, hold with probability at least $1 - 2e^{-\kappa d} - \delta - \epsilon$. Now, first whenever $\|\hat{\mathbf{w}}\| \leq R(\delta)$, we discretize $\hat{\mathbf{w}}$. Let

$$\widehat{\mathcal{W}}(R(\delta), d, \kappa) := \{\hat{\mathbf{w}} \in \mathbb{R}^d \mid \|\hat{\mathbf{w}}\| \leq R(\delta), \|\hat{\mathbf{w}}\|_0 \leq \kappa d\},$$

where $\|\hat{\mathbf{w}}\|_0$ denotes the number of non-zero components of $\hat{\mathbf{w}}$. Assume that $\widetilde{\mathcal{W}}(R(\delta), d, \kappa)$ is a discretization of this space with $v > 0$ precision, i.e. for every $\hat{\mathbf{w}} \in \widehat{\mathcal{W}}(R(\delta), d, \kappa)$, there exists $\tilde{\mathbf{w}} \in \widetilde{\mathcal{W}}(R(\delta), d, \kappa)$ satisfying $\|\tilde{\mathbf{w}} - \hat{\mathbf{w}}\| \leq v$. Among all such coverings, consider the one with minimum number of \mathcal{N}_v points.

Lemma S4. $\mathcal{N}_v \leq e^{dh_b(\kappa)} \left(\frac{3R(\delta)}{v} \right)^{\kappa d}$.

Note that in general $\|\hat{\mathbf{w}}\| \leq \|\mathbf{w}\|$. Let $l := c_1(\delta, \tau) \sqrt{\frac{(\kappa + \epsilon_\kappa)d \log(n)}{n}}$ and $v = \frac{al}{4\mathcal{L}(\tau, \delta)}$, where $a := \frac{12\mathcal{L}(\tau, \delta)R(\delta)}{12\mathcal{L}(\tau, \delta)R(\delta) + \sqrt{d}}$. Then

$$\begin{aligned} &\mathbb{P}\left(|\mathcal{R}_{0,\tau}(\hat{\mathbf{w}}) - \hat{\mathcal{R}}_{0,\tau}(\hat{\mathbf{w}})| \geq l \cup \|\mathbf{w}\| > R(\delta) \cup A^C\right) \\ &\leq \mathbb{P}\left(|\mathcal{R}_{0,\tau}(\hat{\mathbf{w}}) - \hat{\mathcal{R}}_{0,\tau}(\hat{\mathbf{w}})| \geq l \cap \|\mathbf{w}\| \leq R(\delta)\right) + \mathbb{P}(\|\mathbf{w}\| \geq R(\delta)) + \mathbb{P}(A^C) \\ &\leq \mathbb{P}\left(|\mathcal{R}_{0,\tau}(\hat{\mathbf{w}}) - \hat{\mathcal{R}}_{0,\tau}(\hat{\mathbf{w}})| \geq l \cap \|\mathbf{w}\| \leq R(\delta)\right) + \delta + \epsilon \\ &\leq \mathbb{P}\left(\sup_{\hat{\mathbf{w}} \in \widehat{\mathcal{W}}(R(\delta), d, \kappa)} |\mathcal{R}_{0,\tau}(\hat{\mathbf{w}}) - \hat{\mathcal{R}}_{0,\tau}(\hat{\mathbf{w}})| \geq l/2\right) + \delta + \epsilon \\ &\stackrel{(a)}{\leq} \mathbb{P}\left(\max_{\tilde{\mathbf{w}} \in \widetilde{\mathcal{W}}(R(\delta), d, \kappa)} |\mathcal{R}_{0,\tau}(\tilde{\mathbf{w}}) - \hat{\mathcal{R}}_{0,\tau}(\tilde{\mathbf{w}})| \geq l(1-a)/2\right) + \delta + \epsilon \\ &\stackrel{(b)}{\leq} \mathcal{N}_v \max_{\tilde{\mathbf{w}} \in \widetilde{\mathcal{W}}(R(\delta), d, \kappa)} \mathbb{P}\left(|\mathcal{R}_{0,\tau}(\tilde{\mathbf{w}}) - \hat{\mathcal{R}}_{0,\tau}(\tilde{\mathbf{w}})| \geq l(1-a)/2\right) + \delta + \epsilon \\ &\stackrel{(c)}{\leq} 2\mathcal{N}_v \exp(-nl^2(1-a)^2/2) + \delta + \epsilon \\ &\stackrel{(d)}{\leq} 2 \exp\left(-nl^2(1-a)^2/2 + \kappa d \log\left(\frac{12\mathcal{L}(\tau, \delta)R(\delta)}{al}\right) + dh_b(\kappa)\right) + \delta + \epsilon, \quad (\text{S29}) \end{aligned}$$

where (a) is derived since

$$|\mathcal{R}_{0,\tau}(\hat{\mathbf{w}}) - \hat{\mathcal{R}}_{0,\tau}(\hat{\mathbf{w}})| \leq |\mathcal{R}_{0,\tau}(\tilde{\mathbf{w}}) - \hat{\mathcal{R}}_{0,\tau}(\tilde{\mathbf{w}})| + 2\mathcal{L}(\tau, \delta)v = |\mathcal{R}_{0,\tau}(\tilde{\mathbf{w}}) - \hat{\mathcal{R}}_{0,\tau}(\tilde{\mathbf{w}})| + al/2.$$

by Lemma S3, given that $v \leq R/\sqrt{L}$, and the triangle inequality. The inequality (b) is obtained by applying the union bound, (c) is derived using Hoeffding's inequality and since loss is bounded by 1, and (d) is due to Lemma S4.

It remains to show that the term in the exponent in (S29) is upper bounded by $-\kappa d/2$ and $v \leq R/\sqrt{L}$.

$$-nl^2(1-a)^2/2 + \kappa d \log\left(\frac{12\mathcal{L}(\tau, \delta)R(\delta)}{al}\right) + dh_b(\kappa) \quad (\text{S30})$$

$$= -\frac{c_1(\delta, \tau)^2(1-a)^2\kappa d \log(n)}{2} + \frac{\kappa d}{2} \log(n) \quad (\text{S31})$$

$$+ \kappa d \log\left(\frac{12\mathcal{L}(\tau, \delta)R(\delta)}{ac_1(\delta, \tau)\sqrt{d}}\right) \quad (\text{S32})$$

$$- \frac{c_1(\delta, \tau)^2(1-a)^2\epsilon_\kappa d \log(n)}{2} - \frac{\kappa d}{2} \log(\kappa + \epsilon_\kappa) + dh_b(\kappa) \quad (\text{S33})$$

$$- \frac{\kappa d}{2} \log \log(n). \quad (\text{S34})$$

It can be verified that (S31) and (S32) are non-positive when $c_1(\delta, \tau) \geq (12\mathcal{L}(\tau, \delta)R(\delta) + \sqrt{d})/\sqrt{d}$. Moreover, with this choice of $c_1(\delta, \tau)$, (S33) is non-positive for $\epsilon_\kappa = (2h_b(\kappa) - \kappa \log(\kappa))/(\log(n))$. Finally, (S33) is less than $-\kappa d/2$, for $n \geq 16$.

Finally with the chosen value of v , $v \leq R/\sqrt{L}$ holds if $n/\log(n) \geq 10L$. This completes the proof. \square

S5.6 Proof of Corollary 1

For notation convenience, let $\mathcal{S}\alpha\mathcal{S}_n(\sigma) \equiv \mathcal{S}\alpha\mathcal{S}(\sigma_\alpha\sigma)$, where n stands for normalized and $\sigma_\alpha := (2\Gamma(-\alpha)\cos((2-\alpha)\pi/2))^{1/\alpha}$. First, we state the Corollary for a more general case, and then we state the proof of this general result.

Corollary S2. Assume that for $l \in \llbracket 1, L \rrbracket$ and $i \in \llbracket 1, d_l \rrbracket$, the conditional distribution of $w_{l,i} \stackrel{i.i.d.}{\sim} \mathcal{S}\alpha_l\mathcal{S}_n(\sigma_l)$ with $\alpha_l \in (1, 2)$. Further assume that $\sigma^2 := \sum_{l=1}^L (d_l/d)\sigma_l^2$ and $\{\alpha_l\}_{l=1}^L$ do not depend on S . Then for every $\varepsilon > 0$, $\kappa_l \in (0, 1)$, $l \in \llbracket 1, L \rrbracket$, and $\beta > 0$, there exists $d_{l,0} \in \mathbb{N}$, such that for every n : $n/\log(n) \geq 10L$ and $\tau > 0$, with probability at least $1 - 3d^{-\beta}$,

$$\mathcal{R}_0(\hat{\mathbf{w}}) \leq \hat{\mathcal{R}}_\gamma(\mathbf{w}) + \left(a(\alpha)\sigma^L d^{\frac{L(\alpha+2\beta+2)}{2\alpha}}/\tau + \sqrt{d}\right)\sqrt{(\kappa + \epsilon_\kappa)\log(n)/n}, \quad (\text{S35})$$

where $\{\hat{\mathbf{w}}_l\}_l = \{\mathbf{w}_l^{(\kappa d_l)}\}_l$, $\alpha := \min_l \alpha_l$, $a(\alpha) := 6\sqrt{2}B6^L 4^{L/\alpha}/L^{(L-3)/2}$, $\gamma := \tau + b_\varepsilon(\alpha)\sigma^L d^{\frac{L(\alpha+2\beta+2)}{2\alpha}}/\tau$, and $b_\varepsilon(\alpha) := \sqrt{2}B3^L 4^{L/\alpha}((1+\varepsilon)^L - 1)/L^{L/2}$.

Proof. First, given any S , we bound the term $R_S(\delta)$, defined as

$$R_S(\delta) := \inf\{R: \mathbb{P}(\|\mathbf{w}\| \geq R|S) \leq \delta\}. \quad (\text{S36})$$

Lemma S5. If for $l \in \llbracket 1, L \rrbracket$, \mathbf{x}_l is an i.i.d. d_l -dimensional vector with $\mathcal{S}\alpha_l\mathcal{S}_n(\sigma_l)$ distributions and $\alpha_l \in (1, 2)$, then for $\delta < 2d(2 - \max_l \alpha_l)^\alpha$

$$\inf\{R: \mathbb{P}(\|\mathbf{x}\| \geq R) \leq \delta\} \leq 3\sigma\sqrt{d}\left(\frac{4d}{\delta}\right)^{1/\alpha},$$

where $\sigma := \sqrt{\sum_{l=1}^L (d_l/d)\sigma_l^2}$ and $\alpha := \min_l \alpha_l$.

Hence, $R_S(\delta) \leq 3\sigma\sqrt{d}\left(\frac{4d}{\delta}\right)^{1/\alpha}$. Since σ , α , and $\max_l \alpha_l$ do not depend on S , then this bound is the same for all S . Thus, for $\delta < 2d(2 - \max_l \alpha_l)^\alpha$,

$$R(\delta) \leq 3\sigma\sqrt{d}\left(\frac{4d}{\delta}\right)^{1/\alpha}. \quad (\text{S37})$$

Next, due to Lemma S2, the assumption **H 1** holds for any $\varepsilon > 0$ and $\{\kappa_l\}_{l=1}^L: \kappa_l \in (0, 1)$ and some $\{d_{l,0}\}_{l=1}^L: d_{l,0} \in \mathbb{N}$, with $\epsilon = 0$. Note that $d_{l,0}$ does not depend on S as $\{\alpha_l\}_{l=1}^L$ is independent of S . The proof follows now by Theorem 4 with $\delta = d^{-\beta}$ and using the relation (S37) when $2d_0^{\beta+1}(2 - \max_l \alpha_l)^\alpha \geq 1$ and $d_0/\log(d_0) \geq \beta/\kappa$. \square

S5.7 Proof of Theorem S6

Proof. The proof of this theorem is similar to the proof of Theorem 4. Fix $\delta, \tau > 0$. We show that with probability of at least $1 - 2e^{-d/2} - \delta - \epsilon$:

$$\mathcal{R}_{0,\tau}(\mathbf{w}) \leq \hat{\mathcal{R}}_{0,\tau}(\mathbf{w}) + \max\left(2, 24\rho_\epsilon(\kappa, d)\mathcal{L}(\tau, \delta)R(\delta)/\sqrt{d}\right)\sqrt{d\log(n)/n}, \quad (\text{S38})$$

where $\mathcal{R}_{0,\tau}(\cdot)$ and $\hat{\mathcal{R}}_{0,\tau}(\cdot)$ are defined in (S27). The claim follows then by noting that

$$\begin{aligned} \mathcal{R}_0(\mathbf{w}) &\leq \mathcal{R}_{0,\tau}(\mathbf{w}), \\ \hat{\mathcal{R}}_{0,\tau}(\mathbf{w}) &\leq \hat{\mathcal{R}}_\tau(\mathbf{w}), \end{aligned}$$

due to (S27).

Recall that for all $l \in \llbracket 1, L \rrbracket$, $\hat{\mathbf{w}}_l := \mathbf{w}_l^{(\kappa_l d_l)}$. Denote by A the event that \mathbf{w} is compressible, i.e. when for all $l \in \llbracket 1, L \rrbracket$, $\|\hat{\mathbf{w}}_l - \mathbf{w}_l\| \leq \varepsilon \|\mathbf{w}_l\|$. Denote its complement by A^C and note that $\mathbb{P}(A^C) \leq \epsilon$, where the probability is with respect to $P_{\mathbf{w}}$.

In the following, first we discretize \mathbf{w} whenever $\|\mathbf{w}\| \leq R(\delta)$. Let

$$\mathcal{W}(R(\delta), \varepsilon, d, \kappa) := \left\{ \mathbf{w} \in \mathbb{R}^d \mid \|\mathbf{w}\| \leq R(\delta), \|\mathbf{w}^{(\kappa d)} - \mathbf{w}\| \leq \varepsilon R(\delta) \right\}.$$

Assume that $\mathcal{W}'(R(\delta), \varepsilon, d, \kappa)$ is the discretization of this space with $v > 0$ precision, i.e. for every $\mathbf{w} \in \mathcal{W}(R(\delta), \varepsilon, d, \kappa)$, there exists $\mathbf{w}' \in \mathcal{W}'(R(\delta), \varepsilon, d, \kappa)$ satisfying $\|\mathbf{w}' - \mathbf{w}\| \leq v$. Among all such coverings, consider the one with minimum number of \mathcal{N}'_v points.

Lemma S6. For $d \geq 10$, if $v < \varepsilon R(\delta)$, then $\mathcal{N}'_v \leq \left(\frac{3\rho_\epsilon(\kappa, d)R}{v}\right)^d$.

Similar to the proof of Theorem 4 and by letting $l := c_2(\delta, \tau, \kappa)\sqrt{\frac{d\log(n)}{n}}$ and $v = \frac{al}{4\mathcal{L}(\tau, \delta)}$, where $a := \frac{12\rho_\epsilon(\kappa, d)\mathcal{L}(\tau, \delta)R(\delta)}{12\rho_\epsilon(\kappa, d)\mathcal{L}(\tau, \delta)R(\delta) + \sqrt{d}}$,

$$\begin{aligned} &\mathbb{P}\left(|\mathcal{R}_{0,\tau}(\mathbf{w}) - \hat{\mathcal{R}}_{0,\tau}(\mathbf{w})| \geq l\right) \\ &\leq \mathbb{P}\left(|\mathcal{R}_{0,\tau}(\mathbf{w}) - \hat{\mathcal{R}}_{0,\tau}(\mathbf{w})| \geq l \cup \|\mathbf{w}\| > R(\delta) \cup A^C\right) \\ &\leq \mathbb{P}\left(|\mathcal{R}_{0,\tau}(\mathbf{w}) - \hat{\mathcal{R}}_{0,\tau}(\mathbf{w})| \geq l \cap \|\mathbf{w}\| \leq R(\delta) \cap A\right) + \delta + \epsilon \\ &\leq \mathbb{P}\left(\sup_{\mathbf{w} \in \mathcal{W}(R(\delta), \varepsilon, d, \kappa)} |\mathcal{R}_{0,\tau}(\mathbf{w}) - \hat{\mathcal{R}}_{0,\tau}(\mathbf{w})| \geq l/2\right) + \delta + \epsilon \\ &\stackrel{(a)}{\leq} \mathcal{N}'_v \max_{\mathbf{w}' \in \mathcal{W}'(R(\delta), \varepsilon, d, \kappa)} \mathbb{P}\left(|\mathcal{R}_{0,\tau}(\mathbf{w}') - \hat{\mathcal{R}}_{0,\tau}(\mathbf{w}')| \geq l(1-a)/2\right) + \delta + \epsilon \\ &\stackrel{(b)}{\leq} 2 \exp\left(-\frac{nl^2(1-a)^2}{2} + d \log\left(\frac{12\rho_\epsilon(\kappa, d)\mathcal{L}(\tau, \delta)R(\delta)}{al}\right)\right) + \delta + \epsilon, \quad (\text{S39}) \end{aligned}$$

where (a) holds when $v \leq R/\sqrt{L}$ and (b) holds using Lemma S6 if $v < \varepsilon R(\delta)$.

It remains to show that the term in the exponent in (S39) is upper bounded by $-d/2$, $v < \varepsilon R(\delta)$, and $v \leq R/\sqrt{L}$. To show the first claim, we can write

$$-\frac{nl^2(1-a)^2}{2} + d \log\left(\frac{12\rho_\epsilon(\kappa, d)\mathcal{L}(\tau, \delta)R(\delta)}{al}\right) = -\frac{c_2(\delta, \tau, \kappa)^2(1-a)^2 d \log(n)}{2} + \frac{d}{2} \log(n) \quad (\text{S40})$$

$$+ d \log\left(\frac{12\rho_\epsilon(\kappa, d)\mathcal{L}(\tau, \delta)R(\delta)}{ac_2(\delta, \tau, \kappa)\sqrt{d}}\right) \quad (\text{S41})$$

$$- \frac{d}{2} \log \log(n). \quad (\text{S42})$$

It can be verified that (S40) and (S41) are non-positive when $c_2(\delta, \tau, \kappa) = (12\rho_\varepsilon(\kappa, d)\mathcal{L}(\tau, \delta)R(\delta) + \sqrt{d})/\sqrt{d}$ and (S42) is less than $-d/2$, for $n \geq 16$.

To verify $v < \varepsilon R(\delta)$, where $v = \frac{d}{4\mathcal{L}(\tau, \delta)}$, we have

$$\begin{aligned} v &= \frac{12\rho_\varepsilon(\kappa, d)\mathcal{L}(\tau, \delta)R(\delta)}{12\rho_\varepsilon(\kappa, d)\mathcal{L}(\tau, \delta)R(\delta) + \sqrt{d}} \times \frac{12\rho_\varepsilon(\kappa, d)\mathcal{L}(\tau, \delta)R(\delta) + \sqrt{d}}{\sqrt{d}} \times \frac{\sqrt{d\log(n)/n}}{4\mathcal{L}(\tau, \delta)} \\ &= 3\rho_\varepsilon(\kappa, d)R(\delta)\sqrt{\log(n)/n} \\ &\leq 9\varepsilon^{1-\kappa}R(\delta)\sqrt{\log(n)/n} \stackrel{(a)}{\leq} \varepsilon R(\delta), \end{aligned}$$

where (a) holds when $\varepsilon^\kappa \geq 9\sqrt{\log(n)/n}$.

Moreover, with the chosen value of v , $v \leq R/\sqrt{L}$ holds if $n/\log(n) \geq 9L$. Finally note that $(12\rho_\varepsilon(\kappa, d)\mathcal{L}(\tau, \delta)R(\delta) + \sqrt{d}) \leq \max(24\rho_\varepsilon(\kappa, d)\mathcal{L}(\tau, \delta)R(\delta), 2\sqrt{d})$. This completes the proof. \square

S5.8 Proof of Proposition S1

Proof. For ease of notations, for $\kappa, \varepsilon > 0$ and $\mathbf{w} \in \mathbb{R}^d$, let

$$\varepsilon_p(\mathbf{w}, \kappa) := \|\mathbf{w}^{(\kappa d)} - \mathbf{w}\|_p / \|\mathbf{w}\|_p \text{ and hence } \kappa_p(\mathbf{w}, \varepsilon) := \min\{\kappa : \varepsilon_p(\mathbf{w}, \kappa) \leq \varepsilon\}. \quad (\text{S43})$$

Let $\mathbf{x} = (|w_1|, \dots, |w_d|)$ and let $x_{d,i}$ be the corresponding ordered sequence, i.e.

$$x_{d,1} \geq x_{d,2} \geq \dots \geq x_{d,d}.$$

Let

$$\mathbf{y}^d = \frac{1}{a_d}(x_{d,1}, x_{d,2}, \dots, x_{d,d}, 0, 0, \dots) \in \mathbb{R}^\infty,$$

where a_d is a normalizing constant defined in [LWZ81, Equation 3]. Moreover let $e_i, i = 1, 2, \dots$, be i.i.d. standard exponential random variables with partial sum $\Gamma_i := \sum_{l=1}^i e_l$ and let $z_i(\alpha) := \Gamma_i^{-1/\alpha}$. Then, due to [LWZ81, Lemma 1],

$$\lim_{d \rightarrow \infty} \mathbf{y}^d \stackrel{\text{d}}{=} (z_1(\alpha), z_2(\alpha), \dots).$$

where d denotes convergence in distribution.

First, we show that for any $\kappa > 0$, $\varepsilon_p(\mathbf{z}^d(\alpha), \kappa)$ is increasing with respect to α . This term can be written as

$$\varepsilon_p(\mathbf{z}^d(\alpha), \kappa)^p = \frac{\sum_{l=\lceil \kappa d \rceil + 1}^d z_l(\alpha)^p}{\sum_{l=1}^d z_l(\alpha)^p} = \frac{\sum_{l=\lceil \kappa d \rceil + 1}^d \Gamma_l^{-\frac{p}{\alpha}}}{\sum_{l=1}^d \Gamma_l^{-\frac{p}{\alpha}}} =: \frac{u}{v}.$$

Taking the derivative with respect to α gives

$$\frac{\partial \varepsilon_p(\mathbf{z}^d(\alpha), \kappa)^p}{\partial \alpha} = \frac{vu' - v'u}{v^2},$$

where

$$\begin{aligned} vu' - v'u &= \frac{p}{\alpha^2} \left[\left(\sum_{l=1}^d \Gamma_l^{-\frac{p}{\alpha}} \right) \left(\sum_{l=\lceil \kappa d \rceil + 1}^d \Gamma_l^{-\frac{p}{\alpha}} \log(\Gamma_l) \right) - \left(\sum_{l=1}^d \Gamma_l^{-\frac{p}{\alpha}} \log(\Gamma_l) \right) \left(\sum_{l=\lceil \kappa d \rceil + 1}^d \Gamma_l^{-\frac{p}{\alpha}} \right) \right] \\ &= \frac{p}{\alpha^2} \sum_{l_1=1}^{\lceil \kappa d \rceil} \sum_{l_2=\lceil \kappa d \rceil + 1}^d \Gamma_{l_1}^{-\frac{p}{\alpha}} \Gamma_{l_2}^{-\frac{p}{\alpha}} (\log(\Gamma_{l_2}) - \log(\Gamma_{l_1})) \\ &\stackrel{a.s.}{>} 0. \end{aligned}$$

This shows that $\varepsilon_p(\mathbf{z}^d(\alpha), \kappa)$ is almost surely strictly increasing with respect to α , and consequently $\kappa_p(\mathbf{z}^d(\alpha), \varepsilon)$ is almost surely increasing with respect to α .

Since $\varepsilon_p(\mathbf{w}, \kappa)$ is a bounded function and almost surely continuous with respect to \mathbf{w} , $\mathbb{E}[\varepsilon_p(\mathbf{w}_i^d, \kappa)]$ converges also to $\mathbb{E}[\varepsilon_p(\mathbf{z}_i^\infty(\alpha_i), \kappa)]$, for $i = 1, 2$. To show (S6), choose $d_0(\delta)$ large enough, such that

$$\begin{aligned} \left| \mathbb{E}[\varepsilon_p(\mathbf{w}_1^d, \kappa)] - \mathbb{E}[\varepsilon_p(\mathbf{z}_1^\infty(\alpha_1), \kappa)] \right| &< \frac{\delta}{4}, \quad \left| \mathbb{E}[\varepsilon_p(\mathbf{w}_2^d, \kappa)] - \mathbb{E}[\varepsilon_p(\mathbf{z}_2^\infty(\alpha_2), \kappa)] \right| < \frac{\delta}{4}, \\ \left| \mathbb{E}[\varepsilon_p(\mathbf{z}_1^d, \kappa)] - \mathbb{E}[\varepsilon_p(\mathbf{z}_1^\infty(\alpha_1), \kappa)] \right| &< \frac{\delta}{4}, \quad \left| \mathbb{E}[\varepsilon_p(\mathbf{z}_2^d, \kappa)] - \mathbb{E}[\varepsilon_p(\mathbf{z}_2^\infty(\alpha_2), \kappa)] \right| \leq \frac{\delta}{4}. \end{aligned}$$

Then,

$$\mathbb{E}[\varepsilon_p(\mathbf{w}_2^d, \kappa)] - \mathbb{E}[\varepsilon_p(\mathbf{w}_1^d, \kappa)] < \delta + \mathbb{E}[\varepsilon_p(\mathbf{z}_2^d(\alpha_2), \kappa)] - \mathbb{E}[\varepsilon_p(\mathbf{z}_1^d(\alpha_1), \kappa)] < \delta.$$

Similarly, (S7) can be concluded. □

S6 Proofs of the Technical Lemmas

In this section, we give proofs of all the unproved lemmas stated in the paper.

S6.1 Proof of Lemma S1

Proof. Inequality (S3) can be concluded from part i. of Lemma S3, stated in Section S5.5, by letting $v_l = \varepsilon_l \|\mathbf{w}_l\|$. Inequality (S4) can be concluded from (S3) and since when $\|\mathbf{w}\| \leq R$, then

$$\prod_{l=1}^L \|\mathbf{w}_l\| \leq \left(\frac{R}{\sqrt{L}} \right)^L.$$
□

S6.2 Proof of Lemma S3

Proof. i. Similar to [NBS18], we will show the first inequality by induction. Let $f_{\mathbf{w}}^l(\mathbf{x})$ denote the output of the l th layer: $f_{\mathbf{w}}^1(\mathbf{x}) = \mathbf{W}_1 \mathbf{x}$ and $f_{\mathbf{w}}^l(\mathbf{x}) = \mathbf{W}_l \phi(f_{\mathbf{w}}^{l-1}(\mathbf{x}))$. We show that for $i \in \llbracket 1, L \rrbracket$, following relations hold:

$$\|f_{\mathbf{w}}^i(\mathbf{x}) - f_{\mathbf{w}'}^i(\mathbf{x})\| \leq B \prod_{l=1}^i (\|\mathbf{w}_l\| + v_l) - B \prod_{l=1}^i \|\mathbf{w}_l\|.$$

The induction base $i = 0$ holds trivially. Assume that it holds till layer i . We show that it holds for layer $i + 1$ as well. Note that with our notations $\mathbf{w}_l = \text{vec}(\mathbf{W}_l)$ and consequently $\|\mathbf{W}_l\| = \|\mathbf{w}_l\|$.

$$\begin{aligned} &\|f_{\mathbf{w}'}^{i+1}(\mathbf{x}) - f_{\mathbf{w}}^{i+1}(\mathbf{x})\| \\ &= \|\mathbf{W}_{i+1}' \phi(f_{\mathbf{w}'}^i(\mathbf{x})) - \mathbf{W}_{i+1} \phi(f_{\mathbf{w}}^i(\mathbf{x}))\| \\ &= \|(\mathbf{W}_{i+1}' + \mathbf{W}_{i+1}' - \mathbf{W}_{i+1}) (\phi(f_{\mathbf{w}}^i(\mathbf{x})) + \phi(f_{\mathbf{w}'}^i(\mathbf{x})) - \phi(f_{\mathbf{w}}^i(\mathbf{x}))) - \mathbf{W}_{i+1} \phi(f_{\mathbf{w}}^i(\mathbf{x}))\| \\ &\leq \|(\mathbf{W}_{i+1}' - \mathbf{W}_{i+1}) \phi(f_{\mathbf{w}}^i(\mathbf{x}))\| + \|\mathbf{W}_{i+1} (\phi(f_{\mathbf{w}'}^i(\mathbf{x})) - \phi(f_{\mathbf{w}}^i(\mathbf{x})))\| \\ &\quad + \|(\mathbf{W}_{i+1}' - \mathbf{W}_{i+1}) (\phi(f_{\mathbf{w}'}^i(\mathbf{x})) - \phi(f_{\mathbf{w}}^i(\mathbf{x})))\| \\ &\stackrel{(a)}{\leq} v_{i+1} B \prod_{l=1}^i \|\mathbf{w}_l\| + (\|\mathbf{w}_{i+1}\| + v_{i+1}) \left(B \prod_{l=1}^i (\|\mathbf{w}_l\| + v_l) - B \prod_{l=1}^i \|\mathbf{w}_l\| \right) \\ &= B \prod_{l=1}^{i+1} (\|\mathbf{w}_l\| + v_l) - B \prod_{l=1}^{i+1} \|\mathbf{w}_l\|. \end{aligned}$$

where (a) is concluded since ϕ is 1-Lipschitz, $\phi(0) = 0$, and since due to the structure of $f_{\mathbf{w}}$, $\|f_{\mathbf{w}}^i(\mathbf{x})\|$ can be upper bounded as

$$\|f_{\mathbf{w}}^i(\mathbf{x})\| \leq \|\mathbf{x}\| \prod_{l=1}^i \|\mathbf{w}_l\| \leq B \prod_{l=1}^i \|\mathbf{w}_l\|.$$

Next, we show the second inequality.

$$\begin{aligned} |\ell_{0,\tau}(\mathbf{z}, f_{\mathbf{w}}) - \ell_{0,\tau}(\mathbf{z}, f_{\mathbf{w}'})| &\leq \frac{1}{\tau} \left| f_{\mathbf{w}}(\mathbf{x})[y] - \max_{j \neq y} f_{\mathbf{w}}(\mathbf{x})[j] - f_{\mathbf{w}'}(\mathbf{x})[y] + \max_{j' \neq y} f_{\mathbf{w}'}(\mathbf{x})[j'] \right| \\ &\leq \frac{1}{\tau} |f_{\mathbf{w}}(\mathbf{x})[y] - f_{\mathbf{w}'}(\mathbf{x})[y]| + \frac{1}{\tau} \left| \max_{j \neq y} f_{\mathbf{w}}(\mathbf{x})[j] - \max_{j' \neq y} f_{\mathbf{w}'}(\mathbf{x})[j'] \right| \\ &\leq \frac{1}{\tau} |f_{\mathbf{w}}(\mathbf{x})[y] - f_{\mathbf{w}'}(\mathbf{x})[y]| + \frac{1}{\tau} \max_{j \neq y} |f_{\mathbf{w}}(\mathbf{x})[j] - f_{\mathbf{w}'}(\mathbf{x})[j]| \\ &\stackrel{(a)}{\leq} \frac{\sqrt{2}}{\tau} \|f_{\mathbf{w}}(\mathbf{x}) - f_{\mathbf{w}'}(\mathbf{x})\|, \end{aligned}$$

where (a) is derived using the relation $x + y \leq \sqrt{2(x^2 + y^2)}$, for $x, y \in \mathbb{R}_+$.

ii. To show the first inequality, note that due to symmetry, R.H.S. of part i. is maximized when $\|\mathbf{w}_l\| = R/\sqrt{L}$, for $l \in \llbracket 1, L \rrbracket$. Hence,

$$\|f_{\mathbf{w}}(\mathbf{x}) - f_{\mathbf{w}'}(\mathbf{x})\| \leq B \left(\left(\frac{R}{\sqrt{L}} + v \right)^L - \left(\frac{R}{\sqrt{L}} \right)^L \right). \quad (\text{S44})$$

Next, we show that if $a \geq b \geq 0$ and $n \in \mathbb{N}$, then

$$a^n - b^n \leq n(a - b)a^{n-1}. \quad (\text{S45})$$

We show this by induction. It trivially holds for $n = 1$. Suppose that it holds till $n \leq i - 1$. We show that it holds for $n = i$, as well.

– if i is even, then

$$a^i - b^i = \left(a^{\frac{i}{2}} - b^{\frac{i}{2}} \right) \left(a^{\frac{i}{2}} + b^{\frac{i}{2}} \right) \stackrel{(a)}{\leq} \frac{i}{2} (a - b) a^{i/2-1} \times 2a^{i/2} = i(a - b) a^{i-1},$$

where (a) is derived using the induction assumption.

– if i is odd, then

$$a^i - b^i = (a - b) \sum_{k=0}^{i-1} a^k b^{i-1-k} \leq i(a - b) a^{i-1}.$$

Thus, using (S44) and (S45) and since $v \geq R/\sqrt{L}$,

$$\|f_{\mathbf{w}}(\mathbf{x}) - f_{\mathbf{w}'}(\mathbf{x})\| \leq BL \left(\frac{2R}{\sqrt{L}} \right)^{L-1} v.$$

This completes the proof for the first inequality. Finally, the second inequality trivially follows from the first one and part i. □

S6.3 Proof of Lemma S4

Proof. Note that there exists $\binom{d}{\kappa d}$ different ways to choose κd coordinates with zero values. Next, each of the resulting κd -dimensional sub-space can be discretized using at most $\left(\frac{3R(\delta)}{v} \right)^{\kappa d}$ number of points due to [Wu20, Theorem 14.2.]. Using the following lemma completes the proof.

Lemma S7 ([Gal68, Exercise 5.8.b.]). For $n, m \in \mathbb{Z}^+$ and $m \leq n$, $\binom{n}{m} \leq e^{nh_b(m/n)}$. □

S6.4 Proof of Lemma S5

Proof. First we show that in general when random variables $y_i, i \in \llbracket 1, m \rrbracket$ are independent and $\sum_{i=1}^m a_i \leq a$, then

$$\mathbb{P}\left(\sum_{i=1}^m y_i \geq a\right) \leq \sum_{i=1}^m \mathbb{P}(y_i \geq a_i).$$

We prove this for the case of $m = 2$, and the general case follows by an induction.

$$\begin{aligned} \mathbb{P}(y_1 + y_2 \geq a) &= \mathbb{P}(y_1 + y_2 \geq a, y_1 \geq a_1) + \mathbb{P}(y_1 + y_2 \geq a, y_1 < a_1) \\ &\leq \mathbb{P}(y_1 \geq a_1) + \mathbb{P}(y_1 + y_2 \geq a, y_1 < a_1) \\ &\leq \mathbb{P}(y_1 \geq a_1) + \mathbb{P}(y_2 \geq a - a_1, y_1 < a_1) \\ &\leq \mathbb{P}(y_1 \geq a_1) + \mathbb{P}(y_2 \geq a_2). \end{aligned}$$

Next, since stable distributions are continuous distributions, hence $P(\|\mathbf{x}\| \geq R(\delta)) = \delta$.

Now, to show the idea, first show that if \mathbf{x} is an i.i.d. d -dimensional vector with $\mathcal{S}\alpha\mathcal{S}_n(\sigma)$ distributions and $\alpha \in (1, 2)$, then for $\delta < 2d(2 - \alpha)^\alpha$, $R(\delta)$ can be bounded as

$$R(\delta) \leq 3\sigma\sqrt{d}\left(\frac{4d}{\delta}\right)^{1/\alpha}. \quad (\text{S46})$$

To show this,

$$\begin{aligned} \delta = P(\|\mathbf{x}\|^2 \geq R^2(\delta)) &\leq \sum_{i=1}^d P(\|\mathbf{x}_i\|^2 \geq R^2(\delta)/d) \\ &= \sum_{i=1}^d P(\|\mathbf{x}_i\| \geq R(\delta)/\sqrt{d}) \stackrel{(a)}{\leq} 4d\left(\frac{3\sigma\sqrt{d}}{R(\delta)}\right)^\alpha, \end{aligned} \quad (\text{S47})$$

where (a) holds when $R(\delta) \geq 4\sigma\sqrt{d}/(2 - \alpha)$ due to the following inequality from [BLM20, Theorem 19]. The result is stated for a $\mathcal{S}\alpha\mathcal{S}(\sigma_\alpha) \equiv \mathcal{S}\alpha\mathcal{S}_n(1)$ distribution, where $\sigma_\alpha := (2\Gamma(-\alpha)\cos((2 - \alpha)\pi/2))^{1/\alpha}$. Here, we state the result for arbitrary $\mathcal{S}\alpha\mathcal{S}_n(\sigma)$. If $y \sim \mathcal{S}\alpha\mathcal{S}_n(\sigma)$ and $\alpha \in (1, 2)$, then for $a \geq 4\sigma/(2 - \alpha)$

$$\mathbb{P}(y \geq a) \leq \frac{16}{3}\left(\frac{2\sigma}{a}\right)^\alpha \leq 4\left(\frac{3\sigma}{a}\right)^\alpha.$$

Re-arranging (S47) and considering the condition $R(\delta) \geq 4\sigma\sqrt{d}/(2 - \alpha)$, yields

$$R(\delta) \leq \max\left(3\sigma\sqrt{d}\left(\frac{4d}{\delta}\right)^{1/\alpha}, \frac{4\sigma\sqrt{d}}{(2 - \alpha)}\right).$$

Hence, (S46) holds, at least when

$$3\sigma\sqrt{d}\left(\frac{4d}{\delta}\right)^{1/\alpha} \geq \frac{4\sigma\sqrt{d}}{(2 - \alpha)},$$

which is satisfied when $\delta < 2d(2 - \alpha)^\alpha$.

Now, to show the lemma, let $a_l := d\sigma^2/\sigma_l^2$. Then, similar steps concludes

$$\delta \leq \sum_{l=1}^L \sum_{i=1}^{d_l} \mathbb{P}\left(\|x_{l,i}\| \geq \frac{R(\delta)}{\sqrt{a_l}}\right) \stackrel{(a)}{\leq} 4 \sum_{l=1}^L \sum_{i=1}^{d_l} \left(\frac{3\sigma\sqrt{d}}{R(\delta)}\right)^{\alpha_l} \stackrel{(b)}{\leq} 4d\left(\frac{3\sigma\sqrt{d}}{R(\delta)}\right)^\alpha, \quad (\text{S48})$$

where (a) holds when $R(\delta) \geq \max_l 4\sigma\sqrt{d}/(2 - \alpha_l)$ and (b) holds when $R(\delta) \geq 3\sigma\sqrt{d}$. Note that $3\sigma\sqrt{d} \leq 4\sigma\sqrt{d}/(2 - \alpha_l)$. Finally, similarly, (S46) holds if $\delta < 2d(2 - \max_l \alpha_l)^\alpha$.

□

S6.5 Proof of Lemma S6

Proof. To upper bound \mathcal{N}'_v , first consider the space \mathcal{W}'' , defined as⁵

$$\begin{aligned}\mathcal{W}'' &:= \bigcup_{\substack{\mathcal{A} \\ |\mathcal{A}|=\kappa d}} \mathcal{W}''_{\mathcal{A}}, \\ \mathcal{W}''_{\mathcal{A}} &:= \{\mathbf{w} \in \mathbb{R}^d \mid \|\mathbf{w}_{\mathcal{A}}\| \leq R(\delta), \|\mathbf{w}_{\mathcal{A}^c}\| \leq \varepsilon R(\delta)\}.\end{aligned}$$

Since each of $\mathcal{W}''_{\mathcal{A}}$ is a convex space, then if $v < \varepsilon R(\delta)$, by [Wu20, Theorem 14.2.], it can be discretized with v -precision using at most

$$\begin{aligned}\left(\frac{3}{v}\right)^d \frac{\text{Vol}(\mathcal{W}''_{\mathcal{A}})}{\text{Vol}(\mathbb{B}_d)} &= \left(\frac{3}{v}\right)^d \frac{\frac{\pi^{\kappa d/2} R^{\kappa d}}{\Gamma(\kappa d/2+1)} \times \frac{\pi^{(1-\kappa)d/2} (\varepsilon R)^{(1-\kappa)d}}{\Gamma((1-\kappa)d/2+1)}}{\frac{\pi^{d/2} R^d}{\Gamma(d/2+1)}} \\ &= \left(\frac{3\varepsilon^{(1-\kappa)} R}{v}\right)^d \frac{\Gamma(d/2+1)}{\Gamma(\kappa d/2+1)\Gamma((1-\kappa)d/2+1)},\end{aligned}$$

number of points, where \mathbb{B}_d is the d -dimensional unit ball. Now, since $\mathcal{W}(R(\delta), \varepsilon, d, \kappa) \subseteq \mathcal{W}''$,

$$\begin{aligned}\mathcal{N}'_v &\leq \binom{d}{\kappa d} \left(\frac{3\varepsilon^{(1-\kappa)} R}{v}\right)^d \frac{\Gamma(d/2+1)}{\Gamma(\kappa d/2+1)\Gamma((1-\kappa)d/2+1)}, \\ &\stackrel{(a)}{\leq} e^{d(h_b(\kappa)+h_b^{(1)}(\kappa))} \left(\frac{3\varepsilon^{(1-\kappa)} R}{v}\right)^d \\ &\stackrel{(b)}{=} \left(\frac{3\rho_\varepsilon(\kappa, d) R}{v}\right)^d,\end{aligned}\tag{S49}$$

where (a) is concluded from Lemma S7 and the following lemma and (b) is concluded since one way to discretize $\mathcal{W}(R(\delta), \varepsilon, d, \kappa)$ is to consider the whole sphere with radius R , which needs at most $(3R/v)^d$, due to [Wu20, Theorem 14.2.].

Lemma S8. For $n, m \in \mathbb{Z}^+$, $n \geq m$, and $n \geq 10$,

$$\frac{\Gamma(n/2+1)}{\Gamma(m/2+1)\Gamma((n-m)/2+1)} \leq e^{\lceil n/2 \rceil \max(h_b(\lceil m/2 \rceil / \lceil n/2 \rceil), h_b(\lfloor m/2 \rfloor / \lceil n/2 \rceil))}.$$

□

S6.6 Proof of Lemma S8

Proof. For $m = 0$ or $m = n$, the claim holds with equality. Let $1 \leq m \leq n-1$. When n and m are even, then the lemma can be concluded from Lemma S7. Assume, at least one of n and m are odd numbers. We consider two cases of n being odd and even separately.

Note that for $a \in \mathbb{N}$, [Rob55]

$$\Gamma(a+1) = \sqrt{2\pi a} a^a e^{-a} e^{r_a},\tag{S50}$$

where $1/(12a+1) < r_a < 1/(12a)$. Moreover,

$$\Gamma\left(a + \frac{1}{2}\right) = \frac{\sqrt{\pi}(2a)!}{4^a a!} \stackrel{(*)}{=} \sqrt{2\pi} a^a e^{-a} e^{s_a},\tag{S51}$$

where $(*)$ is derived using (S50) with s_a being bounded as

$$\frac{1}{24a+1} - \frac{1}{12a} < s_a < \frac{1}{24a} - \frac{1}{12a+1}.$$

⁵For a set $\mathcal{A} = \{i_1, \dots, i_r\} \subseteq \llbracket 1, d \rrbracket$, denote $\mathbf{x}_{\mathcal{A}} := (x_{i_1}, x_{i_2}, \dots, x_{i_r})$.

Odd n : Let $n = 2k + 1$ and $m = 2q$, where $1 < q \leq k$. Then,

$$\begin{aligned} \frac{\Gamma(n/2 + 1)}{\Gamma(m/2 + 1)\Gamma((n - m)/2 + 1)} &\stackrel{(a)}{=} \frac{e^{s_{k+1} - (r_q + s_{k+1-q})} (k + 1)^{k+1}}{\sqrt{2\pi q} q^q (k + 1 - q)^{k+1-q}} \\ &\stackrel{(b)}{\leq} \frac{(k + 1)^{k+1}}{q^q (k + 1 - q)^{k+1-q}} \\ &< e^{(k+1)h_b(q/(k+1))} \\ &< e^{\lceil n/2 \rceil \max(h_b(m/2 \lceil n/2 \rceil), h_b(m/2 \lfloor n/2 \rfloor))}, \end{aligned} \quad (\text{S52})$$

where (a) is derived using (S50) and (S51), and (b) is derived, since

$$\begin{aligned} s_{k+1} - (r_q + s_{k+1-q}) &< \frac{1}{24k + 24} - \frac{1}{12k + 13} - \frac{1}{12q + 1} - \frac{1}{24(k - q) + 25} + \frac{1}{12(k - q) + 12} \\ &\leq \frac{1}{24k + 24} - \frac{1}{12k + 13} - \frac{1}{12k + 1} - \frac{1}{25} + \frac{1}{12} \\ &< \frac{1}{12} - \frac{1}{25} \leq 0.05. \end{aligned}$$

The case of m being odd is similar.

Even n : Let $n = 2k$ and $m = 2q + 1$, where $1 < q < k$ and $k \geq 5$. Then,

$$\begin{aligned} \frac{\Gamma(n/2 + 1)}{\Gamma(m/2 + 1)\Gamma((n - m)/2 + 1)} &\stackrel{(a)}{=} \frac{e^{1+r_k - (s_{q+1} + s_{k-q})} \sqrt{k} k^k}{\sqrt{2\pi} (q + 1)^{q+1} (k - q)^{k-q}} \\ &\stackrel{(b)}{<} \frac{1.17\sqrt{k} k^k}{(q + 1)^{q+1} (k - q)^{k-q}} \end{aligned} \quad (\text{S53})$$

where (a) is derived using (S50) and (S51) and (b) is derived since

$$\begin{aligned} r_k - (s_{q+1} + s_{k-q}) &< \frac{1}{12k} - \frac{1}{24q + 25} + \frac{1}{12q + 12} - \frac{1}{24(k - q) + 1} + \frac{1}{12(k - q)} \\ &\leq \frac{1}{6k} - \frac{1}{24k + 1} - \frac{1}{25} + \frac{1}{12} \\ &< 0.07, \end{aligned}$$

where the last step holds for $k \geq 5$.

Next, for $k \geq 5$, either $q + 1 \geq 1.17\sqrt{k}$ or $k - q \geq 1.17\sqrt{k}$. Otherwise, we would conclude $k + 1 < 2.34\sqrt{k}$, which is a contradiction for $k \geq 5$.

– If $q + 1 \geq 1.17\sqrt{k}$, then (S53) is upper bounded by

$$\begin{aligned} \frac{1.17\sqrt{k} k^k}{(q + 1)^{q+1} (k - q)^{k-q}} &\leq \frac{k^k}{(q + 1)^q (k - q)^{k-q}} \\ &\leq \frac{k^k}{q^q (k - q)^{k-q}} \\ &\leq e^{kh_b(q/k)} = e^{\frac{n}{2} h_b(2\lfloor m/2 \rfloor / n)}. \end{aligned}$$

– If $k - q \geq 1.17\sqrt{k}$, then (S53) is upper bounded by

$$\begin{aligned} \frac{1.17\sqrt{k} k^k}{(q + 1)^{q+1} (k - q)^{k-q}} &\leq \frac{k^k}{(q + 1)^{q+1} (k - q)^{k-q-1}} \\ &\leq \frac{k^k}{(q + 1)^{q+1} (k - q - 1)^{k-q-1}} \\ &\leq e^{kh_b((q+1)/k)} = e^{\frac{n}{2} h_b(2\lceil m/2 \rceil / n)}. \end{aligned}$$

□